

---

# Purifying Shampoo: Investigating Shampoo’s Heuristics by Decomposing its Preconditioner

---

**Runa Eschenhagen\***  
Department of Engineering  
University of Cambridge  
re393@cam.ac.uk

**Aaron Defazio**  
Fundamental AI Research  
Meta Platforms, Inc.  
adefazio@meta.com

**Tsung-Hsien Lee**  
AI and Systems Co-Design  
Meta Platforms, Inc.  
zong@meta.com

**Richard E. Turner**  
Department of Engineering  
University of Cambridge  
The Alan Turing Institute  
ret26@cam.ac.uk

**Hao-Jun Michael Shi**  
AI and Systems Co-Design  
Meta Platforms, Inc.  
hjms@meta.com

## Abstract

The recent success of Shampoo in the AlgoPerf contest has sparked renewed interest in Kronecker-factorization-based optimization algorithms for training neural networks. Despite its success, Shampoo relies heavily on several heuristics such as learning rate grafting and stale preconditioning to achieve performance at-scale. These heuristics increase algorithmic complexity, necessitate further hyperparameter tuning, and lack theoretical justification. This paper investigates these heuristics from the angle of Frobenius norm approximation to full-matrix Adam and decouples the preconditioner’s eigenvalues and eigenbasis updates. We show that grafting from Adam mitigates the staleness and mis-scaling of the preconditioner’s *eigenvalues* and how correcting the eigenvalues directly can eliminate the need for learning rate grafting. To manage the error induced by infrequent *eigenbasis* computations, we propose an adaptive criterion for determining the eigenbasis computation frequency motivated by terminating a warm-started QR algorithm. This criterion decouples the update frequency of different preconditioner matrices and enables us to investigate the impact of approximation error on convergence. These practical techniques offer a principled angle towards removing Shampoo’s heuristics and developing improved Kronecker-factorization-based training algorithms.

## 1 Introduction

Structured non-diagonal, and especially Kronecker-factored, preconditioned stochastic gradient algorithms for training neural networks have been extensively studied in the machine learning community (Heskes, 2000; Martens, 2010; Martens & Grosse, 2015; Li, 2018; Gupta et al., 2018). Despite promising results, diagonal methods like Adam and its variants have remained the de facto methods for training neural networks over the past decade (Duchi et al., 2011; Kingma & Ba, 2015). Recently, a distributed implementation of the Shampoo algorithm (Gupta et al., 2018; Anil et al., 2020; Shi et al., 2023) won the external tuning track of the AlgoPerf neural network training algorithm competition (Dahl et al., 2023; Kasimbeg et al., 2025).<sup>1</sup> This has spurred renewed interest in non-

---

\*Work performed while an intern and visiting researcher at FAIR, Meta Platforms.

<sup>1</sup>The *external tuning* track requires a submission to specify a hyperparameter search space, in contrast to the hyperparameter-free *self-tuning* track.

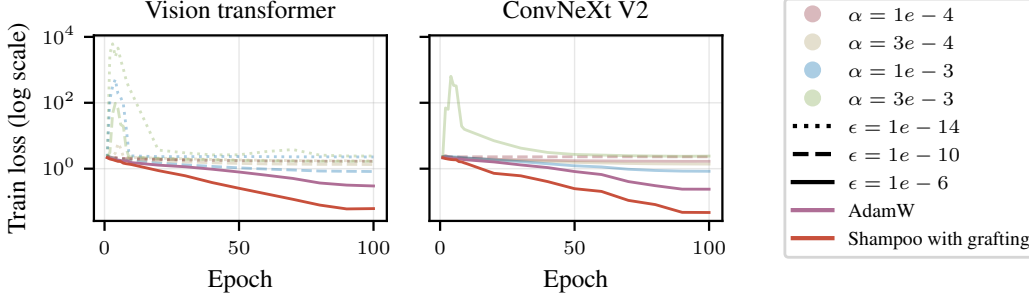


Figure 1: Shampoo with stale preconditioner (updating the root inverse matrices every  $F = 100$  steps) without grafting for different choices of the learning rate  $\alpha$  and  $\epsilon$  on Imagenet. All tested hyperparameter combinations underperform AdamW and, by extension, Shampoo with Adam grafting.

diagonal neural network training algorithms, including new methods like Muon (Jordan et al., 2024; Bernstein, 2025) and SOAP (Vyas et al., 2025).

The winning Shampoo submission to the AlgoPerf competition depended on multiple crucial heuristics on top of the Shampoo algorithm (Anil et al., 2020; Shi et al., 2023). In particular, the update of each layer is re-scaled by the update magnitude of a reference optimizer, also known as *learning rate grafting* (Agarwal et al., 2020); see Figure 1 for an illustration of the importance of the heuristic. Additionally, to amortize the computational overhead, the root-inverse of the preconditioner is only periodically re-computed every 100 steps, resulting in the use of a *stale* preconditioner. However, both heuristics lack theoretical justification and have not been thoroughly understood.

In this paper, we investigate the role of these two heuristics by decoupling the updates of the preconditioner’s eigenvalues and eigenbasis. In Section 3, we empirically demonstrate that Shampoo requires learning rate grafting in order to address the staleness and mis-scaling of the preconditioner’s *eigenvalues*. Correcting Shampoo’s eigenvalues at every step, *à la* SOAP (Vyas et al., 2025), removes the need for grafting. We make this intuition more mathematically precise by comparing bounds on the magnitude of the Shampoo and full-matrix Adam updates. Given the importance of controlling the approximation error of the eigenvalues, we turn to the choice of the *eigenbasis* update frequency in Section 4. Motivated by a termination criterion for a QR algorithm that bounds the relative error of the Kronecker factor approximation induced by the current eigenbasis (Golub & Van Loan, 2013), we show how to adaptively determine the eigenbasis update frequency. We empirically demonstrate that the approximation error of the Kronecker factors evolves and impacts convergence depending on the stage of training and the properties of the parameters. Using an adaptive criterion may increase training efficiency in cases where more frequent eigenbasis computations notably improve convergence in steps.

## 2 Background

We consider neural network training as a standard stochastic optimization problem, where we seek to minimize the expected loss function

$$\min_{\theta \in \mathbb{R}^d} \mathcal{L}(\theta) = \mathbb{E}_{(\mathbf{x}, \mathbf{y}) \sim p_{\mathcal{D}}(\mathbf{x}, \mathbf{y})} [\ell(f_{\theta}(\mathbf{x}), \mathbf{y})], \quad (1)$$

where  $f_{\theta} : \mathbb{R}^N \rightarrow \mathbb{R}^c$  is the neural network prediction function with parameters  $\theta \in \mathbb{R}^d$  flattened and concatenated into a vector,  $p_{\mathcal{D}}(\mathbf{x}, \mathbf{y})$  is the joint data distribution from which inputs  $\mathbf{x} \in \mathbb{R}^N$  and targets  $\mathbf{y} \in \mathbb{R}^c$  are sampled, and  $\ell : \mathbb{R}^c \times \mathbb{R}^c \rightarrow \mathbb{R}$  is the loss function. The neural network is commonly trained using preconditioned stochastic gradient methods that update the parameters at each iteration  $t$  by

$$\theta_t = \theta_{t-1} - \alpha_t \mathbf{C}_t^{-p} \mathbf{g}_t = \theta_{t-1} - \alpha_t \mathbf{Q}_{\mathbf{C}_t} \Lambda_{\mathbf{C}_t}^{-p} \mathbf{Q}_{\mathbf{C}_t}^{\top} \mathbf{g}_t, \quad (2)$$

where  $\mathbf{g}_t = \nabla_{\theta} \ell(f_{\theta_t}(\mathbf{x}_t), \mathbf{y}_t) \in \mathbb{R}^d$  is the stochastic (mini-batch) gradient with respect to sample  $(\mathbf{x}_t, \mathbf{y}_t) \sim p_{\mathcal{D}}(\mathbf{x}, \mathbf{y})$ ,  $\alpha_t > 0$  is the step size, and  $\mathbf{C}_t \in \mathbb{R}^{d \times d}$  is a symmetric positive-definite *preconditioner* or *scaling* matrix. The second equality in Equation (2) expresses the update using the

eigendecomposition of the preconditioner matrix  $C_t = Q_{C_t} \Lambda_{C_t} Q_{C_t}^\top$ , where the eigenbasis matrix  $Q_{C_t} \in \mathbb{R}^{d \times d}$  is orthogonal and eigenvalue matrix  $\Lambda_{C_t} \in \mathbb{R}^{d \times d}$  is diagonal.

We focus on  $C_t$  as an accumulation of gradient outer products, i.e.,  $\bar{A}_t = \sum_{s=1}^t g_s g_s^\top$  or  $A_t = \beta_2 A_{t-1} + (1 - \beta_2) g_t g_t^\top$ , which correspond to full-matrix Adagrad and RMSprop/Adam, respectively (Duchi et al., 2011; Kingma & Ba, 2015). We can also consider alternatives like the Fisher information matrix (Amari, 1998); see Appendix A. When  $C_t$  is diagonal, this scaling recovers simplified versions of popular algorithms like AdaGrad (Duchi et al., 2011) or Adam (Kingma & Ba, 2015), ignoring additional modifications like exponential moving averages, momentum, bias corrections, etc. However, when  $C_t$  is non-diagonal, these preconditioned methods require storing and possibly inverting dense  $d \times d$  matrices, which is prohibitive in practice.

To mitigate this high cost, two structured approximations are commonly applied: (1) a layer-wise block-diagonal approximation, where each block captures pairwise correlations within each layer; (2) a Kronecker product approximation that takes a  $mn \times mn$  matrix block for each layer and re-writes it as a Kronecker product of two smaller matrices of size  $m \times m$  and  $n \times n$ , and has convenient properties for computing the inverse-root matrix-vector product. Notable examples include Kronecker-Factored Approximate Curvature (K-FAC) (Heskes, 2000; Martens & Grosse, 2015; Grosse & Martens, 2016; Martens et al., 2018; Eschenhagen et al., 2023), Shampoo (Gupta et al., 2018; Anil et al., 2020; Shi et al., 2023), and their variants (George et al., 2018; Gao et al., 2020; Ren & Goldfarb, 2021; Feinberg et al., 2023; Duvvuri et al., 2024; Lin et al., 2024b,a). Alternative approaches, such as Hessian-free or inexact Newton methods, avoid explicitly storing the preconditioner matrix, e.g., by leveraging Hessian-vector products (Martens, 2010; Li, 2018; Pooladzandi & Li, 2024).

## 2.1 Shampoo

The Shampoo preconditioner was originally developed as a Kronecker-factorized upper bound to full-matrix Adagrad in its regret analysis (Gupta et al., 2018). For a weight matrix  $W_t \in \mathbb{R}^{m \times n}$  with stochastic gradient  $G_t \in \mathbb{R}^{m \times n}$  where  $g_t = \text{vec}(G_t)$ , Shampoo stores symmetric positive semi-definite matrices that approximate an *idealized* preconditioner with  $L_t \approx \mathbb{E}[G_t G_t^\top] \in \mathbb{R}^{m \times m}$  and  $R_t \approx \mathbb{E}[G_t^\top G_t] \in \mathbb{R}^{n \times n}$ , and updates the preconditioner and weight matrix by

$$L_t = \beta_2 L_{t-1} + (1 - \beta_2) G_t G_t^\top, \quad (3)$$

$$R_t = \beta_2 R_{t-1} + (1 - \beta_2) G_t^\top G_t, \quad (4)$$

$$W_t = W_{t-1} - \alpha_t L_t^{-\frac{1}{4}} G_t R_t^{-\frac{1}{4}} \quad (5)$$

given  $\beta_2 \in [0, 1)$ .<sup>23</sup> Note that the original Shampoo algorithm uses a sum to accumulate over the gradient outer products, although the exponential moving average form as presented here is more commonly used in practice. Therefore, we are interested in approximating the preconditioner of full-matrix Adam given by  $A_t = \beta_2 A_{t-1} + (1 - \beta_2) g_t g_t^\top \approx \mathbb{E}[g_t g_t^\top]$ .

The search direction or update in matrix form is given as  $U_t^{\text{Shampoo}} = -L_t^{-\frac{1}{4}} G_t R_t^{-\frac{1}{4}}$ . Equivalently, we can set  $C_t^{\text{Shampoo}} = (R_t \otimes L_t)^{\frac{1}{2}}$  and  $p = 1/2$  in Equation (2). This update rule can also be generalized to higher-order weight tensors. We will also consider *Shampoo*<sup>2</sup> defined as  $C_t^{\text{Shampoo}^2} = R_t \otimes L_t$ , which is a tighter approximation to full-matrix Adagrad (Morwani et al., 2025).

## 2.2 Eigenvalue-corrected Shampoo and SOAP

By leveraging a Kronecker product approximation, Shampoo’s preconditioner is restricted to a Kronecker product structure for both its eigenvectors and eigenvalues. Specifically, if we have a matrix  $C_t = R_t \otimes L_t$  with eigendecompositions  $L_t = Q_{L_t} \Lambda_{L_t} Q_{L_t}^\top$  and  $R_t = Q_{R_t} \Lambda_{R_t} Q_{R_t}^\top$ , then  $C_t$  has eigendecomposition  $C_t = (Q_{R_t} \otimes Q_{L_t})(\Lambda_{R_t} \otimes \Lambda_{L_t})(Q_{R_t} \otimes Q_{L_t})^\top$ . Preconditioning  $-g_t$  with  $C_t^{-p}$  in its matrix form is equivalent to the matrix transformation:

$$U_t^{\text{Shampoo}} = -L_t^{-\frac{1}{4}} G_t R_t^{-\frac{1}{4}} = -Q_{L_t} \Lambda_{L_t}^{-\frac{1}{4}} (Q_{L_t}^\top G_t Q_{R_t}) \Lambda_{R_t}^{-\frac{1}{4}} Q_{R_t}^\top. \quad (6)$$

<sup>2</sup>We drop the subscript in the expectation, taken with respect to  $(x_t, y_t) \sim p_{\mathcal{D}}(x, y)$ .

<sup>3</sup>A pseudo-inverse that ignores the null space of the matrix or perturbing the matrix by a regularization term  $\epsilon I$  for  $\epsilon > 0$  can be used to handle the symmetric positive semi-definite case.

This can be interpreted as applying a Kronecker-product-based coordinate-wise scaling to a gradient with changed basis, i.e.,  $\tilde{\mathbf{G}}_t = \mathbf{Q}_{L_t}^\top \mathbf{G}_t \mathbf{Q}_{R_t}$ . After scaling, the transformed gradient is converted back to its original basis.

Instead of restricting the eigenvalues to be a Kronecker product, Liu et al. (2018) and George et al. (2018) have proposed *correcting* the eigenvalues by decoupling the scaling from the basis in K-FAC. This involves accumulating a separate scaling matrix  $\mathbf{D}_t \approx \mathbb{E}[\tilde{\mathbf{G}}_t^{\odot 2}] \in \mathbb{R}^{m \times n}$  and using it in lieu of  $\Lambda_{R_t} \otimes \Lambda_{L_t}$ .<sup>4</sup> Anil et al. (2020) remarked that the same correction can also be applied to Shampoo. More recently, Vyas et al. (2025) presented promising empirical results for language models using an instance of eigenvalue-corrected Shampoo (EShampoo) called SOAP, which updates the scaling by  $\mathbf{D}_t = \beta_2 \mathbf{D}_{t-1} + (1 - \beta_2) \tilde{\mathbf{G}}_t^{\odot 2}$ . Since then, SOAP has also been shown to perform well for physics-informed neural networks (Wang et al., 2025) and to reduce outlier features in transformers, which potentially improves quantization (He et al., 2024). See Appendix D.1 for a discussion of the optimal choice of  $\mathbf{D}_t$  in Frobenius norm and how it relates to SOAP.

### 3 Learning rate grafting compensates for Shampoo’s eigenvalues

Originally motivated by decoupling the update magnitude from its direction to account for different implicit learning rate schedules induced by different optimizers, Agarwal et al. (2020) proposed a technique called *learning rate grafting* that combines the layer-wise update of an optimizer with the layer-wise update magnitude from a different optimizer. More precisely in Shampoo, given the Shampoo update  $\mathbf{U}_t^{\text{Shampoo}}$  and the grafting method update  $\mathbf{U}_t^{\text{Grafting}}$  (typically Adam) for a single layer with weight  $\mathbf{W}_t$ , the Shampoo per-layer update is re-scaled as

$$\mathbf{W}_{t+1} = \mathbf{W}_t + \alpha_t \frac{\|\mathbf{U}_t^{\text{Grafting}}\|_F}{\|\mathbf{U}_t^{\text{Shampoo}}\|_F} \mathbf{U}_t^{\text{Shampoo}}. \quad (7)$$

A complete description of Shampoo with Adam grafting is given in Appendix B, Algorithm 2.

As mentioned in Section 2.1, Shi et al. (2023) has claimed that learning rate grafting from a base optimizer like Adam has been crucial to Shampoo’s performance; see also Anil et al. (2020); Kasimbeg et al. (2025). We illustrate this in Figure 1 by showing that independent of the hyperparameter setting, Shampoo without grafting (and updating the root inverse matrices every  $F = 100$  steps) underperforms AdamW, with many hyperparameter settings diverging. Anil et al. (2020) claims that grafting is used to account for differences in magnitude of the eigenspectrum of the Kronecker factors for different layers and the infrequent updates of the Kronecker factors and their inverse roots (see Anil et al. (2020), Appendix G). Despite its practical necessity in Shampoo, grafting’s algorithmic role has not been thoroughly investigated.

Here, we focus on the case of Adam grafting, which was used in conjunction with Shampoo ( $F = 100$ ). This configuration was used in the winning submission to the external tuning track of the AlgoPerf competition (Kasimbeg et al., 2025). Since grafting re-scales the update using the Frobenius norm, we compare the Frobenius norm of the updates of full-matrix and diagonal Adam, Shampoo, and EShampoo. Note that the magnitude of the eigendecomposed update in Equation (2) with Kronecker-factored  $\mathbf{Q}_{C_t} = \mathbf{Q}_{R_t} \otimes \mathbf{Q}_{L_t}$  is determined by the norm of the stochastic gradient  $\mathbf{G}_t$  as well as the eigenvalues of  $\mathbf{C}_t$ , which is formalized in the following lemma.

**Lemma 1.** *Let  $\mathbf{U} = \mathbf{Q}_L (\mathbf{D}^{\odot -p} \odot (\mathbf{Q}_L^\top \mathbf{G} \mathbf{Q}_R)) \mathbf{Q}_R^\top \in \mathbb{R}^{m \times n}$  be the generalized eigendecomposed Kronecker-factored update given by orthogonal matrices  $\mathbf{Q}_L \in \mathbb{R}^{m \times m}$ ,  $\mathbf{Q}_R \in \mathbb{R}^{n \times n}$ , and dense scaling matrix  $\mathbf{D} \in \mathbb{R}^{m \times n}$ . Then we have:*

$$\left( \max_{i,j} \mathbf{D}_{i,j} \right)^{-p} \|\mathbf{G}\|_F \leq \|\mathbf{U}\|_F \leq \left( \min_{i,j} \mathbf{D}_{i,j} \right)^{-p} \|\mathbf{G}\|_F. \quad (8)$$

Lemma 1 generalizes multiple algorithmic cases. Specifically, if  $\mathbf{Q}_L = \mathbf{I} \in \mathbb{R}^{m \times m}$ ,  $\mathbf{Q}_R = \mathbf{I} \in \mathbb{R}^{n \times n}$ , and  $\mathbf{D} = \mathbb{E}[\mathbf{G}^{\odot 2}]$  with  $p = 1/2$ ,  $\mathbf{U}$  gives the idealized Adam update. If  $\mathbf{D} = \Lambda_R \otimes \Lambda_L$  with  $\mathbf{L} = \mathbb{E}[\mathbf{G} \mathbf{G}^\top] = \mathbf{Q}_L \Lambda_L \mathbf{Q}_L^\top$  and  $\mathbf{R} = \mathbb{E}[\mathbf{G}^\top \mathbf{G}] = \mathbf{Q}_R \Lambda_R \mathbf{Q}_R^\top$ , then  $\mathbf{U}$  corresponds to the idealized Shampoo update. Selecting  $\mathbf{D} = \mathbb{E}[(\mathbf{Q}_L^\top \mathbf{G} \mathbf{Q}_R)^{\odot 2}]$  instead yields the idealized EShampoo update.

<sup>4</sup>  $\mathbf{X}^{\odot 2}$  denotes the element-wise square.

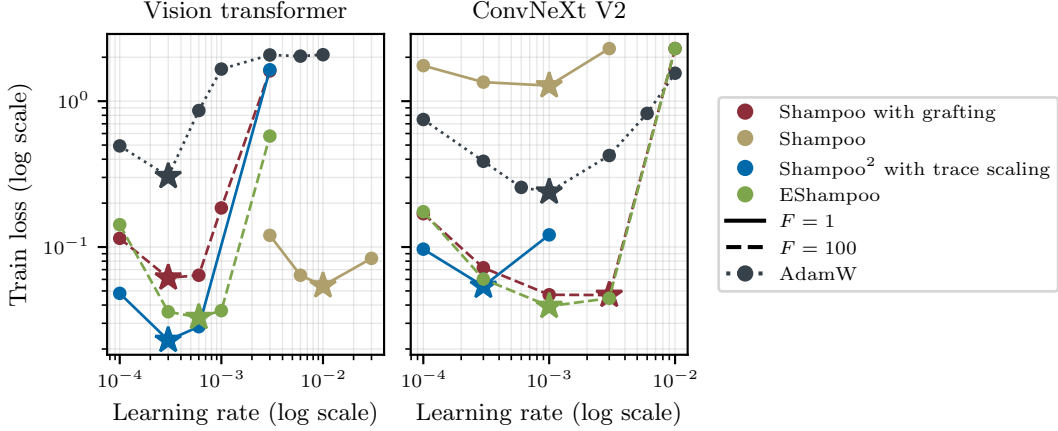


Figure 2: Training results with different Shampoo variants and eigendecomposition frequencies  $F$  on the Imagenet dataset. Shampoo with eigenvalue correction achieves a better training loss compared to Shampoo with Adam grafting, and the optimal learning rate for Adam transfers to both variants.

**Proposition 1.** Assume that  $\mathbb{E}[\mathbf{g}\mathbf{g}^\top]$  is symmetric positive definite. The magnitude of the idealized updates for full-matrix Adam, diagonal Adam, and EShampoo are all bounded by the power of the extreme eigenvalues of full-matrix Adam:

$$\lambda_{\max}(\mathbb{E}[\mathbf{g}\mathbf{g}^\top])^{-p} \|\mathbf{G}\|_F \leq \|\mathbf{U}\|_F \leq \lambda_{\min}(\mathbb{E}[\mathbf{g}\mathbf{g}^\top])^{-p} \|\mathbf{G}\|_F, \quad (9)$$

for all  $p > 0$ . However, under the simplifying assumption that  $\mathbb{E}[\mathbf{G}] = \mathbf{0}$  and  $\mathbf{G}_{i,j}$  is independent from  $\mathbf{G}_{k,l}$  for  $(i,j) \neq (k,l)$  and has bounded second moment,  $\lambda_{\min}(\mathbb{E}[\mathbf{g}\mathbf{g}^\top]) \leq \mathbb{E}[\mathbf{G}_{i,j}^2] \leq \lambda_{\max}(\mathbb{E}[\mathbf{g}\mathbf{g}^\top])$  and Shampoo has dimension-dependent bounds:

$$m^{-p/2} n^{-p/2} \lambda_{\max}(\mathbb{E}[\mathbf{g}\mathbf{g}^\top])^{-p} \|\mathbf{G}\|_F \leq \|\mathbf{U}\|_F \leq m^{-p/2} n^{-p/2} \lambda_{\min}(\mathbb{E}[\mathbf{g}\mathbf{g}^\top])^{-p} \|\mathbf{G}\|_F. \quad (10)$$

This highlights the first potential issue of Shampoo without grafting: the use of stale eigenvalues can result in update magnitudes that lie outside of the bounds of full-matrix Adam. Notably, the basis does not influence the update magnitude. Proposition 1 also suggests that, even in simple settings, Shampoo’s eigenspectrum is mis-scaled relative to Adam’s and EShampoo’s, due to the dependency on the dimensions of the preconditioner. While this additional scaling can be absorbed into the learning rate when only handling a single matrix, it is potentially problematic when one needs to handle multiple parameters simultaneously.

This leads us to the following hypothesis:

The role of learning rate grafting in Shampoo

Learning rate grafting compensates for the staleness and scaling of Shampoo’s eigenvalues.

From the Frobenius norm approximation perspective, we know that  $\mathbf{C}_t^{\text{Shampoo}^2}$  is a tighter approximation to full-matrix Adam compared to  $\mathbf{C}_t^{\text{Shampoo}}$  (Morwani et al., 2025). This directly addresses the mismatch of the eigenvalues’ exponent in Equation (10). Additionally, we can rescale the preconditioner by  $S^{-1} = \text{tr}(\mathbf{R}_t)^{-1} = \text{tr}(\mathbf{L}_t)^{-1}$ , which ensures exactness in the case where full-matrix Adam  $\mathbf{A}_t$  is defined by a single Kronecker product. The scaling  $S^{-1}$  has been previously introduced for Tensor Normal Training (Ren & Goldfarb, 2021, TNT) to approximate the Fisher and is also discussed in Morwani et al. (2025). Naturally, Shampoo<sup>2</sup> with the trace scaling  $S^{-1}$  will have the right scaling when full-matrix Adam can be decomposed into a single Kronecker product.

Based on our observations here, we can make several predictions:

1. By updating Shampoo’s preconditioner at every iteration, we can address the issue of stale eigenvalues. In this scenario, we anticipate that Shampoo without grafting will perform well when the scalings across different layers are relatively consistent, but may struggle when these scalings exhibit substantial discrepancies. This discrepancy is more likely to occur in deep neural networks with highly varying parameter shapes.

2. By using Shampoo<sup>2</sup> with the trace scaling  $S^{-1}C_t^{\text{Shampoo}^2}$  instead of Shampoo  $C_t^{\text{Shampoo}}$  and updating at every iteration, we anticipate that the issues of staleness and scaling may be partially addressed, assuming that full-matrix Adam can nearly decompose into a single Kronecker product. In that case, Shampoo<sup>2</sup> could match Shampoo with grafting.
3. An eigenvalue correction, as used in SOAP, that is updated every iteration also addresses the issues with staleness and scaling, and should match Shampoo with grafting.

**Empirical validation.** To test our predictions, we ablate different settings of Shampoo on the Imagewoof dataset with vision transformer (ViT) and ConvNeXt V2 models. We plot the final training loss after 100 epochs against the learning rate. Following the specification of the AlgoPerf Shampoo submission, we update the preconditioner every 100 steps when grafting the learning rate from Adam, and the eigenbasis when using the eigenvalue correction. Our results are presented in Figure 2. We observe that all three predictions are confirmed. Specifically, Shampoo<sup>2</sup> scaled by  $S^{-1}$  or eigenvalue correction is able to match or even surpass Shampoo with grafting on both problems. Shampoo without grafting can match the final loss for the Imagewoof ViT workload, but not for the ConvNeXt V2 model.

**Hyperparameter transfer.** The optimal learning rate of Adam transfers to Shampoo with grafting and EShampoo. However, it is not completely clear whether the optimal learning rate transfers to Shampoo<sup>2</sup> scaled by  $S^{-1}$ . Learning rate transfer only makes sense when jointly transferring  $\epsilon$  since it affects the effective step size, but Shampoo does not directly add  $\epsilon$  to the root of the eigenvalues, as done in Adam and other diagonal-scaling-based optimizers. While we have not tested this, the optimal learning rate may potentially transfer when matching the effective  $\epsilon$ .

**Computational and memory costs.** While updating Shampoo every iteration incurs a prohibitive computational overhead, the eigenvalue correction is only slightly more expensive than Adam grafting since it requires more matrix multiplications. EShampoo requires the same memory overhead to Shampoo as Adam grafting, specifically requiring an additional  $d$ -dimensional buffer for the second moment accumulation. One could further reduce the memory overhead by leveraging memory-efficient versions of Adam like Adam-mini, which only requires a single scalar for each layer (Zhang et al., 2025b), and could be applied to both grafting as well as the eigenvalue correction.

**Application to other Kronecker-factored methods.** The issue of stale eigenvalues extends to all sparsely-updated Kronecker-factored preconditioners such as K-FAC variants and TNT. Although we are unaware of any work that combines K-FAC or TNT with grafting, it is common practice to apply the Adam update to gradients preconditioned with K-FAC (Pauloski et al., 2021; Osawa et al., 2023a,b; Eschenhagen et al., 2023), which we hypothesize could serve a similar function as grafting.

## 4 Controlling the approximation error induced by stale eigenbases

While we have seen the importance of frequently updating the eigenvalues of the preconditioner in Section 3, we are still unable to predict how much performance we lose by only periodically computing the eigenbasis. The frequency of the eigenbasis computation is often tuned by hand and must be chosen in a problem-dependent way that balances the time of each iteration against the method’s per-iteration convergence rate. Shampoo currently employs a fixed update frequency for all matrices, which does not distinguish between: (1) the stage of training, i.e., the beginning and the end of training; (2) the types of layers, i.e., the first and last layer of the model; and (3) the different Kronecker factors that precondition different dimensions for a single layer, i.e. for  $L$  and  $R$  for the gradient matrix of a linear layer. Furthermore, it does not consider the amount of compute spent on each eigendecomposition, which depends on the parameter shapes.

### 4.1 Can we adaptively control the approximation error induced by the stale eigenbasis?

In the SOAP algorithm, the eigenbasis is computed via an eigendecomposition for the first iteration, and then is subsequently refined by a single step of power iteration followed by a QR decomposition, c.f. Algorithm 4 in Vyas et al. (2025). The authors attribute the application of this method to Wang et al. (2024), Appendix B.<sup>5</sup> The method corresponds to a single iteration of a warm-started simultaneous iteration, an extension of the power iteration for iteratively computing eigendecompositions (Golub &

<sup>5</sup>This approach was referred to as randomized SVD in Wang et al. (2024).

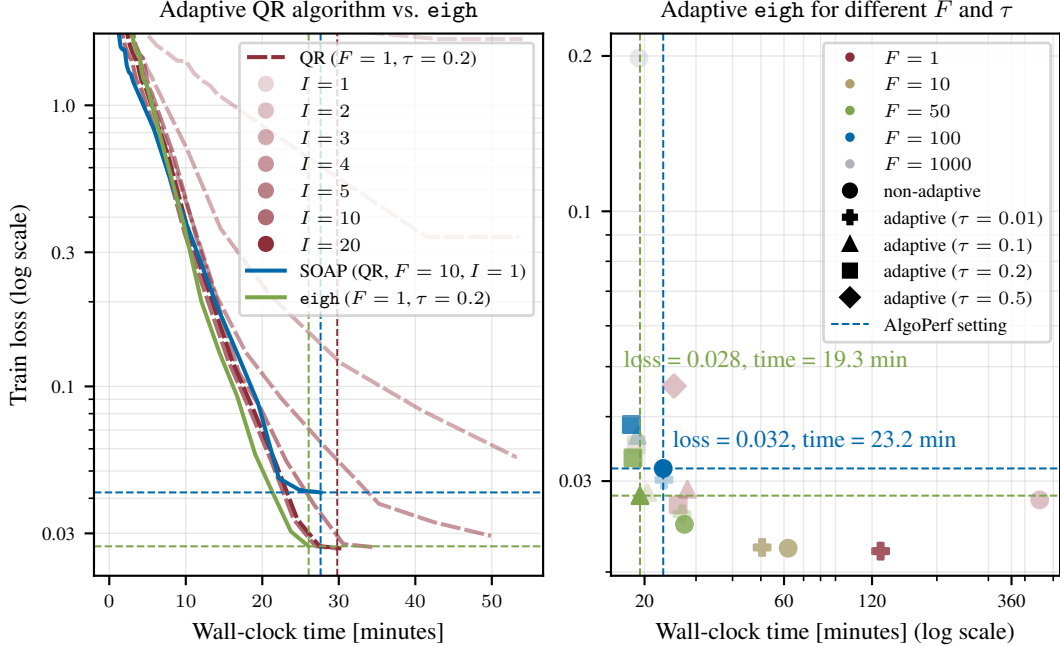


Figure 3: **(left)** On the Imagewoof ViT problem, setting the maximum number of iterations  $I < 10$  with threshold  $\tau = 0.2$  for the adaptive QR algorithm leads to significant increase in wall-clock time compared to using adaptive eigh. Even with  $I = 10$ , adaptive eigh is faster in terms of wall-clock time. The default SOAP setting achieves worse final loss and is also slightly slower. **(right)** Using the adaptive criterion of the QR algorithm to determine when to skip the computation of an eigendecomposition (eigh) improves efficiency by 20% in wall-clock time compared to the AlgoPerf setting of updating every 100 iterations on Imagewoof ViT.

Van Loan, 2013). However, this approach may still yield a poor approximation to the true eigenbasis, especially when it changes rapidly. This depends on the choice of  $\beta_2$  and the dynamics of the stochastic gradient.

Instead, we can control the error induced by the eigenbasis by allowing for multiple iterations of a *warm-started QR algorithm or iteration* to be performed until a relative approximation-error-based convergence criterion is satisfied. There are three major benefits to this approach: (1) each Kronecker factor matrix can be treated independently from others, which decouples the frequency used across different layers, factors, and stages of training; (2) evaluating the criterion with the last computed eigenbasis prior to the first QR algorithm enables us to *skip* eigenbasis updates adaptively; (3) we can control the amount of error we permit in the eigenbasis computation through the choice of the hyperparameter  $\tau \in [0, 1)$ , which quantifies its *inexactness*.

Consider a single Kronecker factor  $L_t \in \mathbb{R}^{m \times m}$  without loss of generality. We want to solve inexactly for an orthogonal matrix  $Q_{L_t}$  such that we obtain an approximation to the eigendecomposition  $L_t = Q_{L_t} \Lambda_{L_t} Q_{L_t}^T$ , with the diagonal eigenvalues matrix  $\Lambda_{L_t}$ . If the previous approximate eigenbasis  $\hat{Q}_{L_{t-1}}$  is a good approximation to the current eigenbasis  $Q_{L_t}$ , then we expect its approximation of the eigenvalues induced by the stale eigenbasis  $\hat{\Lambda}_{L_t} = \hat{Q}_{L_{t-1}}^T L_t \hat{Q}_{L_{t-1}}$  to be nearly diagonal. We can leverage this observation to define a unified criterion for skipping the eigenbasis computation and terminating the warm-started QR algorithm. Diagonalizing the approximate eigenvalues  $\hat{\Lambda}_{L_t}$  produces an approximation to  $L_t$  induced by the stale eigenbasis, specifically,  $\hat{L}_t = \hat{Q}_{L_{t-1}} \text{diag}(\hat{\Lambda}_{L_t}) \hat{Q}_{L_{t-1}}^T$ . Bounding the relative error of this approximation is equivalent to estimating the relative error in the Frobenius norm of the off-diagonal entries of  $\hat{\Lambda}_{L_t}$ , which is cheaper to compute:

Table 1: Results on a subset of the AlgoPerf workloads. We show the mean and standard error of the steps/time to the targets across the runs that reach them. See Appendix E, Table 3 for more results.

Workload	Shampoo Variant	Hits Target	Steps	Time [min]
FastMRI	Adam grafting ( $F = 100$ )	4/5	$4301 \pm 109$	$13.96 \pm 0.44$
	$\mathcal{C}^{\text{EShampoo}}$ ( $F = 100$ )	5/5	$2536 \pm 66$	$10.44 \pm 0.21$
	$\mathcal{C}^{\text{EShampoo}}$ ( $\tau = 0.1, F = 50$ )	5/5	$2468 \pm 145$	$10.81 \pm 0.72$
ImageNet ViT	Adam grafting ( $F = 100$ )	1/1	79907	894.27
	$\mathcal{C}^{\text{EShampoo}}$ ( $F = 100$ )	1/1	76226	894.85
	$\mathcal{C}^{\text{EShampoo}}$ ( $\tau = 0.1, F = 50$ )	1/1	77459	935.89
OGBG	Adam grafting ( $F = 100$ )	2/5	$12574 \pm 708$	$39.20 \pm 1.88$
	$\mathcal{C}^{\text{EShampoo}}$ ( $F = 100$ )	3/5	$8320 \pm 1203$	$33.02 \pm 4.05$
	$\mathcal{C}^{\text{EShampoo}}$ ( $\tau = 0.1, F = 50$ )	5/5	$7117 \pm 328$	$27.55 \pm 3.49$

#### Adaptive eigenbasis computation frequency criterion

$$\frac{\|\mathbf{L}_t - \hat{\mathbf{L}}_t\|_F}{\|\mathbf{L}_t\|_F} = \frac{\|\hat{\mathbf{Q}}_{L_{t-1}}^\top \mathbf{L}_t \hat{\mathbf{Q}}_{L_{t-1}} - \text{diag}(\hat{\mathbf{\Lambda}}_{L_t})\|_F}{\|\hat{\mathbf{Q}}_{L_{t-1}}^\top \mathbf{L}_t \hat{\mathbf{Q}}_{L_{t-1}}\|_F} = \frac{\|\hat{\mathbf{\Lambda}}_{L_t} - \text{diag}(\hat{\mathbf{\Lambda}}_{L_t})\|_F}{\|\hat{\mathbf{\Lambda}}_{L_t}\|_F} \leq \tau. \quad (11)$$

This condition provides a guarantee of the quality of the eigendecomposition approximation. If the condition is satisfied, we set  $\hat{\mathbf{Q}}_{L_t} = \hat{\mathbf{Q}}_{L_{t-1}}$ . Otherwise, we can run the QR algorithm until the condition is satisfied to refine the eigenbasis and set this to  $\hat{\mathbf{Q}}_{L_t}$ . A complete pseudocode of the algorithm is provided in Appendix B, Algorithm 3. Note that evaluating the approximate eigenvalues  $\hat{\mathbf{\Lambda}}_{L_t}$  at the first step requires two matrix multiplications, which is significantly cheaper than computing a step of the QR algorithm.

## 4.2 Does this adaptivity translate to efficiency gains?

The practical efficiency gains of adaptively controlling the approximation error depend on multiple factors. First, the efficiency of the QR algorithm depends heavily on the relative cost of a single QR iteration versus an eigendecomposition, as well as the convergence rate of the QR algorithm, specifically, the number of iterations required to reach a given threshold  $\tau$ . Second, evaluating the criterion adds a constant, albeit small, overhead, independent of the actual frequency of eigendecompositions.

Interestingly, we found that choosing a smaller maximum number of iterations  $I < 10$  in the QR algorithm leads to drastic slowdown in wall-clock time since the total number of QR iterations is larger than the case where we run with a larger budget of  $I \geq 10$  maximum iterations. However, even with a larger number of maximum iterations, the QR algorithm wound up slightly more expensive than computing eigendecompositions with `torch.linalg.eigh` (short: `eigh`) whenever Equation (11) does not hold. The default configuration of SOAP, which computes a single step of the warm-started simultaneous iteration every 10 steps, was also slightly slower in wall-clock time compared to adaptively computing eigendecompositions and reaches a worse final loss. This result conflicts with the observation in Figure 7 in Vyas et al. (2025) that the SOAP setting matches `eigh` when using the same fixed frequency – likely due to the considered language modeling task. See Figure 3 (left).

Therefore, we focus on leveraging the criterion for deciding when to call `eigh`. To potentially bound the total possible number of eigendecompositions performed over the course of training, we evaluate the criterion at a fixed frequency  $F$  as opposed to every step. We ablate different choices of the choice of  $F$  and  $\tau$  in Figure 3 (right). We compare against the baseline setting of the winning AlgoPerf submission, which re-computes the eigendecomposition of all factor matrices every 100 steps on the Imagewoof ViT problem. We observe that this setting without adaptivity requires 20% more wall-clock time compared to an adaptive setting ( $\tau = 0.1, F = 50$ ).

To test whether the results generalize to other problems, we consider a subset of the AlgoPerf workloads and compare the winning Shampoo submission with Adam grafting to: (1) EShampoo with the same fixed eigenbasis computation frequency of  $F = 100$ ; and (2) EShampoo with  $\tau = 0.1$

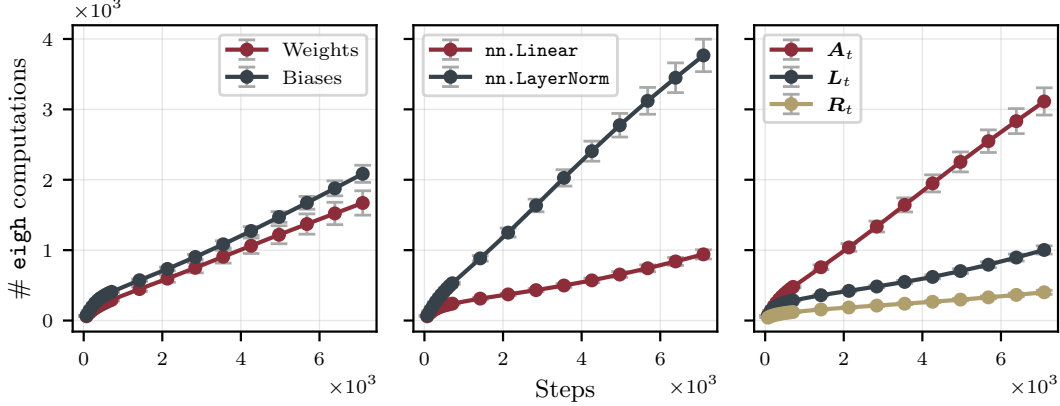


Figure 4: We show the mean with standard error across preconditioners corresponding to the labels in the legends, for  $\tau = 0.01$  and  $F = 1$  on Imagewoof ViT. The eigenbases for biases and layer normalization parameters are changing faster than for weight matrices and linear layers, respectively.

and  $F = 50$ ; see Table 1. First, as predicted by Section 3, EShampoo with the fixed eigenbasis update frequency matches or outperforms Shampoo with Adam grafting in steps and wall-clock time, using the same hyperparameters. Second, using the adaptive criterion with  $\tau = 0.1$  and  $F = 50$  matches the fixed frequency  $F = 100$  for the FastMRI and OGBG workloads, and does slightly worse for ImageNet ViT. We also present results with other fixed and adaptive frequencies in Appendix E, Table 3. Overall, we find that the performance on the considered problems is quite robust to the eigenbasis computation frequency (c.f. Appendix E, Table 3). We expect that when Shampoo’s convergence benefits from more frequent eigenbasis updates, adaptively determining the frequency can result in higher efficiency.

### 4.3 What patterns of adaptivity emerge?

The criterion in Equation (11) also provides a means of measuring how rapidly the preconditioner’s eigenbasis is changing. We examine how many eigendecomposition computations are performed across training steps broken down across different parameter and layer types in our Imagewoof ViT setup. We set  $\tau = 0.01$  and check the condition every iteration ( $F = 1$ ); see Figure 4.

Generally, we observe that more frequent eigendecomposition computations are performed early in training. When comparing weight and bias parameters, we find that the eigenbases of the preconditioners corresponding to the biases evolve more rapidly than for weight matrices. Moreover, the eigenbases for layer normalization parameters change faster than for linear layer parameters, with on average almost  $4\times$  total computations. Finally, we also compare the number of eigendecompositions across the two Kronecker factors  $L_t$  and  $R_t$  for weight matrices, and  $A_t$  for biases and layer normalization parameters.<sup>6</sup> We observe more frequent updating for biases and layer normalization parameters, but it is unclear whether the underlying mechanism is related to the use of full-matrix Adam or some other properties about the training dynamics of the biases and layer normalization parameters. We also find that the eigenbasis is updated more frequently for  $L_t$  compared to  $R_t$ .

### 4.4 How does the error induced by the eigenbasis affect convergence?

While we have investigated the effect of directly controlling the error induced by the preconditioner’s stale eigenbasis, we do not care about this error itself but its impact on convergence. In the Imagewoof ViT setting, we find that the approximation quality (determined by  $\tau$ ) during early iterations is dramatically more important than during later iterations; see Figure 5 (left). Setting  $\tau = 0.8$  for the first 90% and  $\tau = 0.01$  for the last 10% of iterations leads to an identical final loss as  $\tau = 0.8$  for all of training ( $\approx 0.09 - 0.1$ ). In contrast, setting  $\tau = 0.01$  for the first 10% and  $\tau = 0.8$  for the remaining 90% of iterations leads to a significantly lower final loss ( $\approx 0.04$ ). In fact, setting

<sup>6</sup>Full-matrix Adam is also used for weight matrices  $\mathbf{W}_t \in \mathbb{R}^{m \times n}$  with  $mn \leq \text{max\_preconditioner\_dim}$ , which is a hyperparameter to control the largest possible dimension of the preconditioner.

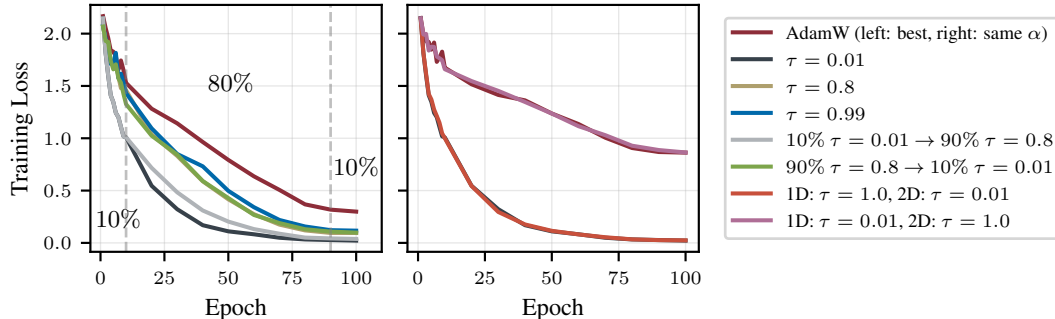


Figure 5: **(left)** The error in the eigenbases is dramatically more important for early iterations. A single eigenbasis computation at the first iteration ( $\tau = 0.99$ ) is sufficient to outperform AdamW. **(right)** The difference between the convergence behavior of AdamW and EShampoo on this problem can be exclusively attributed to the eigenbases corresponding to 2D parameters.

$\tau = 0.99$  for all of training, which effectively computes the eigenbases for the first iteration and then freezes them for the rest of training still significantly outperforms AdamW ( $\approx 0.12$  vs.  $0.3$ ).<sup>7</sup>

Inspired by the discrepancy in the rate of change of the eigenbases corresponding to 1D and 2D parameters (c.f. Figure 4, right), we compare an Imagewoof ViT run with  $\tau = 0.01$  for 2D parameters and no change of basis, i.e. Adam, for 1D parameters and vice versa. Perhaps surprisingly, using Adam for 1D parameters does not affect the convergence behavior and final loss at all. Running Adam for 2D parameters and changing the basis according to  $\tau = 0.01$  for 1D parameters closely matches Adam’s convergence and final loss; see Figure 5 (right).

Considering that the eigenbasis corresponding to 1D parameters is changing much faster than for others and about 45% of the preconditioner matrices correspond to 1D parameters, this means that a large fraction of all eigendecompositions which are computed to respect a fixed threshold  $\tau$  do not impact convergence at all. For example, in this setting, using  $\tau = 0.01$  for all parameters results in a  $2.9\times$  increased runtime compared to only using EShampoo for 2D and Adam for 1D parameters, while achieving the same final loss. In practice, SOAP already uses Adam for 1D parameters, although purely motivated by reducing the computational and memory overhead (Vyas et al., 2025).

## 5 Discussion and conclusion

In this paper, we find that frequently updating the eigenvalues while periodically updating the eigenbasis of Shampoo’s preconditioner provides a principled and practical approach for eliminating grafting. It remains unclear whether the same correction directly applies to the AdaGrad summation, or if a different basis-aware eigenvalue correction is needed (c.f. Appendix D.2). We also show how to control the approximation error induced by the stale eigenbasis, which can improve efficiency. The remaining obstacles to determining the eigenbasis computation frequency independently of the problem are understanding how approximation error affects convergence and integrating systems considerations, such as batched kernel efficiency, into the algorithmic design. Further exploration is needed to understand how these trade-offs evolve with scale, e.g. for large language models.

While our work focuses on Shampoo, the ideas are not limited to the AdaGrad family, and can be adapted to other methods such as K-FAC and TNT. Turning to Shampoo’s theoretical analysis, a key open question is how to integrate approximation quality into Shampoo’s regret bound (c.f. Appendix D.1). Finally, we assume in this work that full-matrix Adam is the ideal algorithm to approximate; however, there are alternative explanations for Shampoo’s effectiveness (Carlson et al., 2015; Benzing, 2022; Bernstein & Newhouse, 2024; Pethick et al., 2025; Zhang et al., 2025a).

<sup>7</sup>For 5 out of 172 Kronecker factors the eigenbasis is computed twice instead of just once.

## Acknowledgments

We thank Anna Cai, Parameswaran Raman, and Ke Sang for their in-depth review of the paper. We are grateful for insightful discussions with Ganesh Ajjanagadde, Rohan Anil, Anna Cai, Rong Jin, Jihao Andreas Lin, Bruno Mlodozeniec, Vinay Rao, Isaac Reid, and Xingyu (Alice) Yang. We also acknowledge managerial support from Yuchen Hao, Guna Lakshminarayanan, Maxim Naumov, Sandeep Parab, Chunqiang Tang, and Lin Xiao. Runa Eschenhagen is supported by ARM, the Cambridge Trust, and the Qualcomm Innovation Fellowship. Richard E. Turner is supported by Google, Amazon, ARM, Improbable and an EPSRC Prosperity Partnership (EP/T005386/1) and the EPSRC Probabilistic AI Hub (EP/Y028783/1).

## References

- Naman Agarwal, Rohan Anil, Elad Hazan, Tomer Koren, and Cyril Zhang. Disentangling adaptive gradient methods from learning rates. arXiv2002.11803, 2020.
- Shun-Ichi Amari. Natural gradient works efficiently in learning. *Neural computation*, 10(2), 1998.
- Kang An, Yuxing Liu, Rui Pan, Shiqian Ma, Donald Goldfarb, and Tong Zhang. ASGO: Adaptive structured gradient optimization. arXiv 2503.20762, 2025.
- Rohan Anil, Vineet Gupta, Tomer Koren, Kevin Regan, and Yoram Singer. Scalable second order optimization for deep learning. arXiv 2002.09018, 2020.
- Frederik Benzing. Gradient descent on neurons and its link to approximate second-order optimization. In *ICML*, 2022.
- Albert S Berahas, Majid Jahani, Peter Richtárik, and Martin Takáč. Quasi-Newton methods for deep learning: Forget the past, just sample. arXiv 1901.09997, 2020.
- Alberto Bernacchia, Mate Lengyel, and Guillaume Hennequin. Exact natural gradient in deep linear networks and its application to the nonlinear case. In *NeurIPS*, 2018.
- Jeremy Bernstein. Deriving Muon, 2025. URL <https://jeremybernste.in/writing/deriving-muon>.
- Jeremy Bernstein and Laker Newhouse. Old optimizer, new norm: An anthology. arXiv 2409.20325, 2024.
- Lucas Beyer, Xiaohua Zhai, and Alexander Kolesnikov. Better plain ViT baselines for ImageNet-1k. arXiv 2205.01580, 2022.
- Raghu Bollapragada, Jorge Nocedal, Dheevatsa Mudigere, Hao-Jun Shi, and Ping Tak Peter Tang. A progressive batching L-BFGS method for machine learning. In *International Conference on Machine Learning*, pp. 620–629. PMLR, 2018.
- Léon Bottou, Frank E Curtis, and Jorge Nocedal. Optimization methods for large-scale machine learning. *SIAM review*, 60(2):223–311, 2018.
- David Carlson, Volkan Cevher, and Lawrence Carin. Stochastic spectral descent for restricted Boltzmann machines. In *ICML*, 2015.
- George E. Dahl, Frank Schneider, Zachary Nado, Naman Agarwal, Chandramouli Shama Sastry, Philipp Hennig, Sourabh Medapati, Runa Eschenhagen, Priya Kasimbeg, Daniel Suo, Juhan Bae, Justin Gilmer, Abel L. Peirson, Bilal Khan, Rohan Anil, Mike Rabbat, Shankar Krishnan, Daniel Snider, Ehsan Amid, Kongtao Chen, Chris J. Maddison, Rakshith Vasudev, Michal Badura, Ankush Garg, and Peter Mattson. Benchmarking neural network training algorithms. arXiv 2306.07179, 2023.
- John Duchi, Elad Hazan, and Yoram Singer. Adaptive subgradient methods for online learning and stochastic optimization. *JMLR*, 12(61), 2011.

- Sai Surya Duvvuri, Fnu Devvrit, Rohan Anil, Cho-Jui Hsieh, and Inderjit S Dhillon. CASPR: Combining axes preconditioners through Kronecker approximation for deep learning. In *ICLR*, 2024.
- Runa Eschenhagen, Alexander Immer, Richard E. Turner, Frank Schneider, and Philipp Hennig. Kronecker-Factored Approximate Curvature for modern neural network architectures. In *NeurIPS*, 2023.
- Vladimir Feinberg, Xinyi Chen, Y. Jennifer Sun, Rohan Anil, and Elad Hazan. Sketchy: Memory-efficient adaptive regularization with frequent directions. In *NeurIPS*, 2023.
- Kai-Xin Gao, Xiaolei Liu, Zheng-Hai Huang, Min Wang, Zidong Wang, Dachuan Xu, and F. Yu. A trace-restricted Kronecker-factored approximation to natural gradient. In *AAAI Conference on Artificial Intelligence*, 2020.
- Thomas George, César Laurent, Xavier Bouthillier, Nicolas Ballas, and Pascal Vincent. Fast approximate natural gradient descent in a Kronecker-factored eigenbasis. In *NeurIPS*, 2018.
- Donald Goldfarb, Yi Ren, and Achraf Bahamou. Practical quasi-Newton methods for training deep neural networks. *Advances in Neural Information Processing Systems*, 33:2386–2396, 2020.
- Gene H Golub and Charles F Van Loan. *Matrix computations*. JHU press, 2013.
- Roger B. Grosse and James Martens. A Kronecker-factored approximate Fisher matrix for convolution layers. In *ICML*, 2016.
- Vineet Gupta, Tomer Koren, and Yoram Singer. Shampoo: Preconditioned stochastic tensor optimization. In *ICML*, 2018.
- Bobby He, Lorenzo Noci, Daniele Paliotta, Imanol Schlag, and Thomas Hofmann. Understanding and minimising outlier features in neural network training. In *NeurIPS*, 2024.
- Tom Heskes. On “natural” learning and pruning in multilayered perceptrons. *Neural Computation*, 12(4), 2000.
- Weihua Hu, Matthias Fey, Marinka Zitnik, Yuxiao Dong, Hongyu Ren, Bowen Liu, Michele Catasta, and Jure Leskovec. Open graph benchmark: Datasets for machine learning on graphs. arXiv 2005.00687, 2021.
- Keller Jordan, Yuchen Jin, Vlado Boza, Jiacheng You, Franz Cesista, Laker Newhouse, and Jeremy Bernstein. Muon: An optimizer for hidden layers in neural networks, 2024. URL <https://kellerjordan.github.io/posts/muon/>.
- Priya Kasimbeg, Frank Schneider, Runa Eschenhagen, Juhan Bae, Chandramouli Shama Sastry, Mark Saroufim, Boyuan Feng, Less Wright, Edward Z. Yang, Zachary Nado, Sourabh Medapati, Philipp Hennig, Michael Rabbat, and George E. Dahl. Accelerating neural network training: An analysis of the AlgoPerf competition. In *ICLR*, 2025.
- Nitish Shirish Keskar and Albert S Berahas. adaqn: An adaptive quasi-Newton algorithm for training RNNs. In *Machine Learning and Knowledge Discovery in Databases: European Conference, ECML PKDD 2016, Riva del Garda, Italy, September 19-23, 2016, Proceedings, Part I 16*, pp. 1–16. Springer, 2016.
- Diederik P Kingma and Jimmy Ba. Adam: A method for stochastic optimization. In *ICLR*, 2015.
- Florian Knoll, Jure Zbontar, Anuroop Sriram, Matthew J. Muckley, Mary Bruno, Aaron Defazio, Marc Parente, Krzysztof J. Geras, Joe Katsnelson, Hersh Chandarana, Zizhao Zhang, Michal Drozdal, Adriana Romero, Michael Rabbat, Pascal Vincent, James Pinkerton, Duo Wang, Nafissa Yakubova, Erich Owens, C. Lawrence Zitnick, Michael P. Recht, Daniel K. Sodickson, and Yvonne W. Lui. fastMRI: A publicly available raw k-space and DICOM dataset of knee images for accelerated MR image reconstruction using machine learning. *Radiology: Artificial Intelligence*, 2(1):e190007, 2020. doi: 10.1148/ryai.2020190007. PMID: 32076662.
- Alex Krizhevsky, Ilya Sutskever, and Geoffrey E Hinton. ImageNet classification with deep convolutional neural networks. In *NIPS*, 2012.

- Frederik Kunstner, Lukas Balles, and Philipp Hennig. Limitations of the empirical Fisher approximation for natural gradient descent. In *NeurIPS*, 2019.
- Xi-Lin Li. Preconditioned stochastic gradient descent. *IEEE Transactions on Neural Networks and Learning Systems*, 29(5), 2018.
- Wu Lin, Felix Dangel, Runa Eschenhagen, Juhan Bae, Richard E. Turner, and Alireza Makhzani. Can we remove the square-root in adaptive gradient methods? a second-order perspective. In *ICML*, 2024a.
- Wu Lin, Felix Dangel, Runa Eschenhagen, Kirill Neklyudov, Agustinus Kristiadi, Richard E. Turner, and Alireza Makhzani. Structured inverse-free natural gradient: Memory-efficient & numerically-stable KFAC for large neural nets. In *ICML*, 2024b.
- Xialei Liu, Marc Masana, Luis Herranz, Joost van de Weijer, Antonio M. López, and Andrew D. Bagdanov. Rotate your networks: Better weight consolidation and less catastrophic forgetting. *ICPR*, 2018.
- James Martens. Deep learning via Hessian-free optimization. In *ICML*, 2010.
- James Martens. New insights and perspectives on the natural gradient method. *JMLR*, 21(146), 2014.
- James Martens and Roger Grosse. Optimizing neural networks with Kronecker-factored approximate curvature. In *ICML*, 2015.
- James Martens, Jimmy Ba, and Matt Johnson. Kronecker-factored curvature approximations for recurrent neural networks. In *ICLR*, 2018.
- Deven Morwani, Itai Shapira, Nikhil Vyas, Eran Malach, Sham Kakade, and Lucas Janson. A new perspective on Shampoo’s preconditioner. In *ICLR*, 2025.
- Kazuki Osawa, Satoki Ishikawa, Rio Yokota, Shigang Li, and Torsten Hoefer. ASDL: A unified interface for gradient preconditioning in PyTorch. arXiv 2305.04684, 2023a.
- Kazuki Osawa, Shigang Li, and Torsten Hoefer. PipeFisher: Efficient training of large language models using pipelining and Fisher information matrices. In Dawn Song, Michael Carbin, and Tianqi Chen (eds.), *MLSys*, 2023b.
- J. Gregory Pauloski, Qi Huang, Lei Huang, Shivaram Venkataraman, Kyle Chard, Ian T. Foster, and Zhao Zhang. KAISA: an adaptive second-order optimizer framework for deep neural networks. In *International Conference for High Performance Computing, Networking, Storage and Analysis (SC21)*, 2021.
- Thomas Pethick, Wanyun Xie, Kimon Antonakopoulos, Zhenyu Zhu, Antonio Silveti-Falls, and Volkan Cevher. Training deep learning models with norm-constrained LMOs. arXiv 2502.07529, 2025.
- Omead Pooladzandi and Xi-Lin Li. Curvature-informed SGD via general purpose lie-group preconditioners. arXiv 2402.04553, 2024.
- Yi Ren and Donald Goldfarb. Tensor normal training for deep learning models. In *NeurIPS*, 2021.
- Thomas Robert, Mher Safaryan, Ionut-Vlad Modoranu, and Dan Alistarh. LDAdam: Adaptive optimization from low-dimensional gradient statistics. arXiv 2410.16103, 2024.
- Hao-Jun Michael Shi, Tsung-Hsien Lee, Shintaro Iwasaki, Jose Gallego-Posada, Zhijing Li, Kaushik Rangadurai, Dheevatsa Mudigere, and Michael Rabbat. A distributed data-parallel PyTorch implementation of the Distributed Shampoo optimizer for training neural networks at-scale. arXiv 2309.06497, 2023.
- DiJia Su, Andrew Gu, Jane Xu, Yuandong Tian, and Jiawei Zhao. GaLore 2: Large-scale LLM pre-training by gradient low-rank projection. arXiv 2504.20437, 2025.

- Nikhil Vyas, Depen Morwani, Rosie Zhao, Mujin Kwun, Itai Shapira, David Brandfonbrener, Lucas Janson, and Sham Kakade. SOAP: Improving and stabilizing Shampoo using Adam. In *ICLR*, 2025.
- Sifan Wang, Ananyae Kumar Bhartari, Bowen Li, and Paris Perdikaris. Gradient alignment in physics-informed neural networks: A second-order optimization perspective. arXiv 2502.00604, 2025.
- Sike Wang, Pan Zhou, Jia Li, and Hua Huang. 4-bit Shampoo for memory-efficient network training. In *NeurIPS*, 2024.
- Sanghyun Woo, Shoubhik Debnath, Ronghang Hu, Xinlei Chen, Zhuang Liu, In So Kweon, and Saining Xie. ConvNeXt V2: Co-designing and scaling ConvNets with masked autoencoders. arXiv 2301.00808, 2023.
- Shuo Xie, Tianhao Wang, Sashank Reddi, Sanjiv Kumar, and Zhiyuan Li. Structured preconditioners in adaptive optimization: A unified analysis. arXiv 2503.10537, 2025.
- Jure Zbontar, Florian Knoll, Anuroop Sriram, Tullie Murrell, Zhengnan Huang, Matthew J. Muckley, Aaron Defazio, Ruben Stern, Patricia Johnson, Mary Bruno, Marc Parente, Krzysztof J. Geras, Joe Katsnelson, Hersh Chandarana, Zizhao Zhang, Michal Drozdal, Adriana Romero, Michael Rabbat, Pascal Vincent, Nafissa Yakubova, James Pinkerton, Duo Wang, Erich Owens, C. Lawrence Zitnick, Michael P. Recht, Daniel K. Sodickson, and Yvonne W. Lui. fastMRI: An open dataset and benchmarks for accelerated MRI. arXiv 1811.08839, 2019.
- Thomas T. Zhang, Behrad Moniri, Ansh Nagwekar, Faraz Rahman, Anton Xue, Hamed Hassani, and Nikolai Matni. On the concurrence of layer-wise preconditioning methods and provable feature learning. In *ICML*, 2025a.
- Yushun Zhang, Congliang Chen, Ziniu Li, Tian Ding, Chenwei Wu, Diederik P. Kingma, Yinyu Ye, Zhi-Quan Luo, and Ruoyu Sun. Adam-mini: Use fewer learning rates to gain more. In *ICLR*, 2025b.
- Jiawei Zhao, Zhenyu Zhang, Beidi Chen, Zhangyang Wang, Anima Anandkumar, and Yuandong Tian. GaLore: Memory-efficient LLM training by gradient low-rank projection. arXiv 2403.03507, 2024.

Table 2: Shampoo variants and their properties.

Shampoo variant	Justified from approximation perspective	Matches grafting in steps	Matches grafting in compute & memory	Learning rate transfer
grafting (Adam)	$\times$	$\checkmark$	$\checkmark$	$\checkmark$
$\mathcal{C}^{\text{Shampoo}}$	$\times$	$\times$	$\times$	$\times$
$S^{-1}\mathcal{C}^{\text{Shampoo}^2}$	$\checkmark$	$\checkmark$	$\times$	?
$\mathcal{C}^{\text{EShampoo}}$	$\checkmark$	$\checkmark$	$\checkmark$	$\checkmark$

## A Connecting full-matrix Adagrad to the Fisher

We can also consider a more general class of preconditioned stochastic gradient methods with other choices of  $\mathcal{C}_t$  and  $p > 0$  that update the parameters at each iteration  $t$  by Equation (2). For example, one could choose  $\mathcal{C}_t$  as approximations of the Hessian  $\nabla^2 \mathcal{L}(\theta)$  via subsampling or secant approximation with  $p = 1$ , which yields the class of *stochastic Newton* or *quasi-Newton* methods (Keskar & Berahas, 2016; Bollapragada et al., 2018; Berahas et al., 2020; Goldfarb et al., 2020). Another common choice is the Fisher information matrix  $\mathbf{F}_t = \mathbb{E}_{\hat{\mathbf{y}} \sim f_\theta(\mathbf{x}), \mathbf{x} \sim p_D(\mathbf{x})} [\nabla_{\theta} \ell(f_\theta(\mathbf{x}), \hat{\mathbf{y}}) \nabla_{\theta} \ell(f_\theta(\mathbf{x}), \hat{\mathbf{y}})^\top]$ , which yields the *natural gradient* or, for common loss functions, *generalized Gauss-Newton method* with  $p = 1$  (Amari, 1998; Martens, 2014). A summary of different methods is provided in Bottou et al. (2018).

By instead summing over per-sample gradient outer products,  $\hat{\mathbf{A}}_t$  can be connected to the empirical Fisher. In general, the empirical Fisher is not expected to be a good approximation of the Fisher information matrix (Kunstner et al., 2019). However, by replacing the accumulation with an expectation over the conditional distribution given by the model  $f_\theta$ , full-matrix AdaGrad can be made equivalent to the Fisher. This equivalence reveals a natural extension of Shampoo to approximate the Fisher, called Tensor Normal Training (Ren & Goldfarb, 2021, TNT), and is closely related to the K-FAC preconditioner (Anil et al., 2020). In fact, both approximations are exactly equivalent to the (block-diagonal) Fisher for simple cases such as deep linear networks (also with weight sharing) and mean squared error loss (Bernacchia et al., 2018; Eschenhagen et al., 2023; Morwani et al., 2025). The modifications in TNT deviate from the original Shampoo update (Gupta et al., 2018) because it was motivated by upper bounds to full-matrix AdaGrad in its non-smooth, nonconvex regret analysis, rather than this Fisher approximation perspective.

## B Algorithms pseudocode

In this section, we provide the pseudocode for all algorithms, including eigenvalue-corrected Shampoo (Algorithm 1), Shampoo with Adam grafting (Algorithm 2), and the adaptive warm-started QR algorithm (Algorithm 3). Algorithm 1 and Algorithm 2 present simplified versions of the algorithm ignoring common modifications like momentum or an exponential moving average over the stochastic gradient, bias corrections, and weight decay.

Note that different instances of eigenvalue-corrected Shampoo can be employed by changing the exponential moving average in Equation (13), eigenbasis computation in Equation (14), or eigenvalue correction update in Equation (15). For example, SOAP delays the update of the eigenbasis until after the update step, and approximates the eigenvalue correction (Equation (15)) by

$$\mathbf{D}_t = \beta_2 \mathbf{D}_{t-1} + (1 - \beta_2) \tilde{\mathbf{G}}_t^{\odot 2} \quad (12)$$

and uses a single iteration of the warm-started simultaneous iteration.

## C Proofs

We provide complete proofs for all lemmas, propositions, and corollaries in the paper.

**Lemma 2.** Let  $\mathbf{U} = \mathbf{Q}_L (\mathbf{D}^{\odot -p} \odot (\mathbf{Q}_L^\top \mathbf{G} \mathbf{Q}_R)) \mathbf{Q}_R^\top \in \mathbb{R}^{m \times n}$  be the generalized eigendecomposed Kronecker-factored update given by orthogonal matrices  $\mathbf{Q}_L \in \mathbb{R}^{m \times m}$ ,  $\mathbf{Q}_R \in \mathbb{R}^{n \times n}$ , and dense

---

**Algorithm 1** Idealized eigenvalue-corrected Shampoo (EShampoo) pseudocode

---

**Require:** Parameter  $\mathbf{W}_1 \in \mathbb{R}^{m \times n}$ , learning rate  $\alpha_t > 0$ ,  $\epsilon > 0$ .

- 1: Initialize  $\mathbf{L}_0 = \mathbf{0} \in \mathbb{R}^{m \times m}$ ,  $\mathbf{R}_0 = \mathbf{0} \in \mathbb{R}^{n \times n}$ , and  $\mathbf{D} = \mathbf{0} \in \mathbb{R}^{m \times n}$ .
- 2: **for**  $t = 1, \dots, T$  **do**
- 3:   Compute (mini-batch) stochastic gradient:  $\mathbf{G}_t = \nabla_{\theta} \ell(f_{\theta_t}(\mathbf{x}), \mathbf{y})$ .
- 4:   Update factor matrices:

$$\mathbf{L}_t = \beta_2 \mathbf{L}_{t-1} + (1 - \beta_2) \mathbf{G}_t \mathbf{G}_t^{\top}, \quad \mathbf{R}_t = \beta_2 \mathbf{R}_{t-1} + (1 - \beta_2) \mathbf{G}_t^{\top} \mathbf{G}_t. \quad (13)$$

- 5:   Compute or approximate orthonormal eigenbasis of the factor matrices:

$$\mathbf{\Lambda}_{\mathbf{L}_t}, \mathbf{Q}_{\mathbf{L}_t} = \text{eig}(\mathbf{L}_t), \quad \mathbf{\Lambda}_{\mathbf{R}_t}, \mathbf{Q}_{\mathbf{R}_t} = \text{eig}(\mathbf{R}_t). \quad (14)$$

- 6:   Transform gradient basis:  $\tilde{\mathbf{G}}_t = \mathbf{Q}_{\mathbf{L}_t}^{\top} \mathbf{G}_t \mathbf{Q}_{\mathbf{R}_t}$ .
- 7:   Compute or update eigenvalue correction:

$$\mathbf{D}_t^* = \arg \min_{\mathbf{D} \in \mathbb{R}^{m \times n}} \|\mathbf{A}_t - (\mathbf{Q}_{\mathbf{R}_t} \otimes \mathbf{Q}_{\mathbf{L}_t}) \text{diag}(\text{vec}(\mathbf{D})) (\mathbf{Q}_{\mathbf{R}_t} \otimes \mathbf{Q}_{\mathbf{L}_t})\|_F. \quad (15)$$

- 8:   Compute update:  $\mathbf{W}_{t+1} = \mathbf{W}_t - \alpha_t \mathbf{Q}_{\mathbf{L}_t} (\tilde{\mathbf{G}}_t / (\sqrt{\mathbf{D}_t^*} + \epsilon \mathbf{1}\mathbf{1}^{\top})) \mathbf{Q}_{\mathbf{R}_t}$ .
  - 9: **end for**
- 

---

**Algorithm 2** Shampoo with Adam grafting pseudocode

---

**Require:** Parameter  $\mathbf{W}_1 \in \mathbb{R}^{m \times n}$ , learning rate  $\alpha_t > 0$ , exponential moving average constant  $\beta_2 \in (0, 1)$ ,  $\epsilon > 0$ .

- 1: Initialize  $\mathbf{L}_0 = \mathbf{0} \in \mathbb{R}^{m \times m}$ ,  $\mathbf{R}_0 = \mathbf{0} \in \mathbb{R}^{n \times n}$ , and  $\mathbf{D} = \mathbf{0} \in \mathbb{R}^{m \times n}$ .
- 2: **for**  $t = 1, \dots, T$  **do**
- 3:   Compute (mini-batch) stochastic gradient:  $\mathbf{G}_t = \nabla_{\theta} \ell(f_{\theta_t}(\mathbf{x}), \mathbf{y})$ .
- 4:   Update factor matrices:

$$\mathbf{L}_t = \beta_2 \mathbf{L}_{t-1} + (1 - \beta_2) \mathbf{G}_t \mathbf{G}_t^{\top}, \quad \mathbf{R}_t = \beta_2 \mathbf{R}_{t-1} + (1 - \beta_2) \mathbf{G}_t^{\top} \mathbf{G}_t.$$

- 5:   Update Adam grafting state:  $\mathbf{D}_t = \beta_2 \mathbf{D}_{t-1} + (1 - \beta_2) \mathbf{G}_t^{\odot 2}$ .
- 6:   Compute matrix root inverse of the factor matrices:

$$\mathbf{L}_t^{-1/4} = \text{rootinv}(\mathbf{L}_t), \quad \mathbf{R}_t^{-1/4} = \text{rootinv}(\mathbf{R}_t).$$

- 7:   Compute update:  $\mathbf{W}_{t+1} = \mathbf{W}_t - \alpha_t \frac{\|\mathbf{G}_t / (\sqrt{\mathbf{D}_t} + \epsilon \mathbf{1}\mathbf{1}^{\top})\|_F}{\|\mathbf{L}_t^{-1/4} \mathbf{G}_t \mathbf{R}_t^{-1/4}\|_F} \mathbf{L}_t^{-1/4} \mathbf{G}_t \mathbf{R}_t^{-1/4}$ .
  - 8: **end for**
- 

---

**Algorithm 3** Warm-started QR iteration with relative error termination criterion.

---

**Require:** Matrix  $\mathbf{L} = \mathbf{L}_t$ , previous eigenbasis  $\hat{\mathbf{Q}} = \hat{\mathbf{Q}}_{\mathbf{L}_{t-1}}$ , relative tolerance  $\tau \in [0, 1)$ , maximum number of iterations  $I$ .

- 1:  $i \leftarrow 0$
  - 2:  $\hat{\mathbf{\Lambda}} \leftarrow \hat{\mathbf{Q}}^{\top} \mathbf{L} \hat{\mathbf{Q}}$
  - 3: **while**  $\|\hat{\mathbf{\Lambda}} - \text{diag}(\hat{\mathbf{\Lambda}})\|_F \leq \tau \|\hat{\mathbf{\Lambda}}\|_F$  and  $i < I$  **do**
  - 4:    $\mathbf{Q}, \mathbf{R} \leftarrow \text{QR}(\hat{\mathbf{\Lambda}})$
  - 5:    $\hat{\mathbf{\Lambda}} \leftarrow \mathbf{R} \mathbf{Q}$
  - 6:    $\hat{\mathbf{Q}} \leftarrow \hat{\mathbf{Q}} \mathbf{Q}$
  - 7:    $i \leftarrow i + 1$
  - 8: **end while**
  - 9: **return**  $\hat{\mathbf{Q}}, \hat{\mathbf{\Lambda}}$
-

scaling matrix  $D \in \mathbb{R}^{m \times n}$ . Then we have:

$$(\max_{i,j} D_{i,j})^{-p} \|\mathbf{G}\|_F \leq \|\mathbf{U}\|_F \leq (\min_{i,j} D_{i,j})^{-p} \|\mathbf{G}\|_F. \quad (16)$$

*Proof.* Since the Frobenius norm of a matrix is invariant to orthogonal transformations and the entries of  $D$  are bounded, i.e.,  $\min_{i,j} D_{i,j} \leq D_{i,j} \leq \max_{i,j} D_{i,j}$ , we can show that

$$\begin{aligned} \|\mathbf{U}\|_F &= \|\mathbf{Q}_L(D^{\odot -p} \odot (\mathbf{Q}_L^T \mathbf{G} \mathbf{Q}_R)) \mathbf{Q}_R^T\|_F \\ &= \|D^{\odot -p} \odot (\mathbf{Q}_L^T \mathbf{G} \mathbf{Q}_R)\|_F \\ &\in [(\max_{i,j} D_{i,j})^{-p}, (\min_{i,j} D_{i,j})^{-p}] \cdot \|\mathbf{Q}_L^T \mathbf{G} \mathbf{Q}_R\|_F \\ &\in [(\max_{i,j} D_{i,j})^{-p}, (\min_{i,j} D_{i,j})^{-p}] \cdot \|\mathbf{G}\|_F, \end{aligned}$$

as desired.  $\square$

**Proposition 2.** Assume that  $\mathbb{E}[\mathbf{g}\mathbf{g}^T]$  is symmetric positive definite. The magnitude of the updates for full-matrix Adam, diagonal Adam, and eigenvalue-corrected Shampoo are all bounded by the power of the extreme eigenvalues of full-matrix Adam:

$$\lambda_{\max}(\mathbb{E}[\mathbf{g}\mathbf{g}^T])^{-p} \|\mathbf{G}\|_F \leq \|\mathbf{U}\|_F \leq \lambda_{\min}(\mathbb{E}[\mathbf{g}\mathbf{g}^T])^{-p} \|\mathbf{G}\|_F, \quad (17)$$

for all  $p > 0$ . However, under the simplifying assumption that  $\mathbb{E}[\mathbf{G}] = \mathbf{0}$  and  $\mathbf{G}_{i,j}$  is independent from  $\mathbf{G}_{k,l}$  for  $(i,j) \neq (k,l)$  and has bounded second moment,  $\lambda_{\min}(\mathbb{E}[\mathbf{g}\mathbf{g}^T]) \leq \mathbb{E}[\mathbf{G}_{i,j}^2] \leq \lambda_{\max}(\mathbb{E}[\mathbf{g}\mathbf{g}^T])$  and Shampoo has dimension-dependent bounds:

$$m^{-p/2} n^{-p/2} \lambda_{\max}(\mathbb{E}[\mathbf{g}\mathbf{g}^T])^{-p} \|\mathbf{G}\|_F \leq \|\mathbf{U}\|_F \leq m^{-p/2} n^{-p/2} \lambda_{\min}(\mathbb{E}[\mathbf{g}\mathbf{g}^T])^{-p} \|\mathbf{G}\|_F. \quad (18)$$

*Proof.* Note that Equation (17) holds for full-matrix Adam since  $\|\mathbf{U}\|_F = \|\mathbf{u}\|_2 = \|\mathbb{E}[\mathbf{g}\mathbf{g}^T]^{-p} \mathbf{g}\|_2 \in [\lambda_{\max}(\mathbb{E}[\mathbf{g}\mathbf{g}^T])^{-p}, \lambda_{\min}(\mathbb{E}[\mathbf{g}\mathbf{g}^T])^{-p}] \cdot \|\mathbf{g}\|_2$ , where  $\mathbf{u} = \text{vec}(\mathbf{U})$  and  $\mathbf{g} = \text{vec}(\mathbf{G})$ .

For diagonal Adam and eigenvalue-corrected Shampoo, it is sufficient to show that  $\lambda_{\min}(\mathbb{E}[\mathbf{g}\mathbf{g}^T]) \leq D_{i,j} \leq \lambda_{\max}(\mathbb{E}[\mathbf{g}\mathbf{g}^T])$  for all  $i,j$  and apply Lemma 2. To see this, note that  $D_{i,j}$  can be represented by a Rayleigh quotient, i.e.,

$$D_{i,j} = \mathbb{E}[\mathbf{G}_{i,j}^2] = \mathbf{e}_{i,j}^T \mathbb{E}[\mathbf{g}\mathbf{g}^T] \mathbf{e}_{i,j} \quad (\text{Adam})$$

$$D_{i,j} = \mathbb{E}[(\mathbf{Q}_L^T \mathbf{G} \mathbf{Q}_R)_{i,j}^2] = \mathbf{e}_{i,j}^T (\mathbf{Q}_R \otimes \mathbf{Q}_L)^T \mathbb{E}[\mathbf{g}\mathbf{g}^T] (\mathbf{Q}_R \otimes \mathbf{Q}_L) \mathbf{e}_{i,j} \quad (\text{EShampoo})$$

where  $\mathbf{e}_{i,j} = \text{vec}(\mathbf{E}_{i,j}) \in \mathbb{R}^{mn}$  and  $\mathbf{E}_{i,j} \in \mathbb{R}^{m \times n}$  with

$$(\mathbf{E}_{i,j})_{k,l} = \begin{cases} 1 & \text{if } (k,l) = (i,j) \\ 0 & \text{otherwise.} \end{cases}$$

Since  $\|\mathbf{e}_{i,j}\|_2 = \|(\mathbf{Q}_R \otimes \mathbf{Q}_L) \mathbf{e}_{i,j}\|_2 = 1$ , the desired bound by the extreme eigenvalues follows from the Courant–Fischer–Weyl min-max theorem.

To prove Equation (18), observe that under independence between components of the gradient  $\mathbf{G}_{i,j}$ , the preconditioner for full-matrix Adam  $\mathbb{E}[\mathbf{g}\mathbf{g}^T]$  is a diagonal matrix whose diagonal entries consist of  $\mathbb{E}[\mathbf{G}_{i,j}^2]$  for all  $i,j$ . Hence,  $\mathbb{E}[\mathbf{G}_{i,j}^2]$  is bounded by the minimum and maximum eigenvalues, i.e.,  $\mathbb{E}[\mathbf{G}_{i,j}^2] \in [\lambda_{\min}(\mathbb{E}[\mathbf{g}\mathbf{g}^T]), \lambda_{\max}(\mathbb{E}[\mathbf{g}\mathbf{g}^T])]$ .

Due to independence,  $\mathbb{E}[\mathbf{G}\mathbf{G}^T]$  and  $\mathbb{E}[\mathbf{G}^T \mathbf{G}]$  are also diagonal. Expanding their diagonal entries gives

$$\begin{aligned} (\mathbb{E}[\mathbf{G}\mathbf{G}^T])_{i,i} &= \sum_{j=1}^n \mathbb{E}[\mathbf{G}_{i,j}^2] \in n \cdot [\lambda_{\min}(\mathbb{E}[\mathbf{g}\mathbf{g}^T]), \lambda_{\max}(\mathbb{E}[\mathbf{g}\mathbf{g}^T])] \quad \forall i = 1, \dots, m, \\ (\mathbb{E}[\mathbf{G}^T \mathbf{G}])_{j,j} &= \sum_{i=1}^m \mathbb{E}[\mathbf{G}_{i,j}^2] \in m \cdot [\lambda_{\min}(\mathbb{E}[\mathbf{g}\mathbf{g}^T]), \lambda_{\max}(\mathbb{E}[\mathbf{g}\mathbf{g}^T])] \quad \forall j = 1, \dots, n. \end{aligned}$$

Therefore, the Shampoo preconditioner  $(\mathbb{E}[\mathbf{G}\mathbf{G}^T] \otimes \mathbb{E}[\mathbf{G}^T \mathbf{G}])^{1/2}$  is also diagonal with eigenvalues lying in the interval  $[m^{1/2} n^{1/2} \lambda_{\min}(\mathbb{E}[\mathbf{g}\mathbf{g}^T]), m^{1/2} n^{1/2} \lambda_{\max}(\mathbb{E}[\mathbf{g}\mathbf{g}^T])]$ . The desired result follows.  $\square$

Note that more general bounds can be derived by relaxing the assumption  $\mathbb{E}[\mathbf{G}] = \mathbf{0}$ , although the bounds are more complex and are not more conceptually informative.

## D On the gap between the optimal and practical eigenvalue correction

Eigenvalue-corrected Shampoo shares similarities with memory-efficient optimizers such as GaLore, which apply Adam in a low-dimensional subspace spanned by the largest singular vectors of the gradient matrix (Zhao et al., 2024; Su et al., 2025). However, GaLore relies on the assumption that the gradient resides in a low-rank subspace that evolves gradually, allowing the same optimizer state to be used even as the subspace is updated. A recent method called LDAdam proposed by Robert et al. (2024) describes a projection-aware method that corrects the scaling matrix through both a projection-aware update and generalized error feedback mechanism when transitioning between subspaces to address this issue. We will see that the naive eigenvalue correction as used in SOAP suffers from similar limitations.

### D.1 Optimal eigenvalue correction in Frobenius norm

Note that we can determine the optimal eigenvalue correction by minimizing its Frobenius norm approximation to full-matrix AdaGrad or Adam:

**Proposition 3.** *Given symmetric matrix  $C \in \mathbb{R}^{d \times d}$  and orthogonal matrix  $Q \in \mathbb{R}^{d \times d}$ , the optimal eigenvalue correction  $D^*$  that minimizes the Frobenius norm distance is given by:*

$$D^* := \text{diag}(Q^T C Q) \in \arg \min_{D \in \mathbb{D}^d} \|C - Q D Q^T\|_F. \quad (19)$$

The exact expression for  $D^*$  depends on the form of accumulation used for computing  $C$ ; note that the damping term is omitted here since it does not change the optimal solution.  $T$  denotes the current iteration.

1. (Idealized) If  $C = \mathbb{E}[g g^T]$ , then  $D^* = \mathbb{E}[\text{diag}(Q^T g)^{\odot 2}]$  (George et al., 2018).
2. (AdaGrad) If  $C = \sum_{t=1}^T g_t g_t^T$ , then  $D_T^* = \sum_{t=1}^T \text{diag}(Q_T^T g_t)^{\odot 2}$ .
3. (Adam) If  $C = (1 - \beta_2) \sum_{t=1}^T \beta_2^{T-t} g_t g_t^T$ , then  $D_T^* = (1 - \beta_2) \sum_{t=1}^T \beta_2^{T-t} \text{diag}(Q_T^T g_t)^{\odot 2}$ . Note that  $C$  can be generated recursively via an exponential moving average  $C_T = \beta_2 C_{T-1} + (1 - \beta_2) g_T g_T^T$  with  $C_0 = \mathbf{0} \in \mathbb{R}^{mn \times mn}$ .

*Proof.* (Informal.) Since  $Q$  is orthogonal,  $\|C - Q D Q^T\|_F = \|Q^T C Q - D\|_F$ , with  $D$  diagonal. Therefore, the optimal solution has the form  $D^* = \text{diag}(Q^T C Q)$ . Each case then follows by observing that  $C$  is the expectation or weighted sum of  $g g^T$ , and passing  $Q$  into the sum or expectation.  $\square$

While  $D^*$  is optimal in this sense, it does not guarantee anything regarding the similarity of the (root) inverse of the approximation. Using Proposition 3, we can establish the following corollary.

**Corollary 1.** *The optimal eigenvalue correction yields a tighter Frobenius norm approximation than Shampoo and CASPR, i.e.,*

$$\|C - Q D^* Q^T\|_F \leq \min\{\|C - C^{\text{Shampoo}}\|_F, \|C - C^{\text{CASPR}}\|_F\},$$

where  $C^{\text{CASPR}}$  is the preconditioner used by the CASPR algorithm (Duvvuri et al., 2024).

*Proof.* (Informal.) The first inequality trivially follows from Proposition 3 since by definition the eigenvectors of Shampoo are equal to  $Q = (Q_R \otimes Q_L)^T$ . The second inequality follows from Proposition 3 together with Lemma 3.4 in Duvvuri et al. (2024), which states that the eigenvectors of  $C^{\text{Shampoo}}$  and  $C^{\text{CASPR}}$  are identical.  $\square$

This means that, in the sense of the Frobenius norm approximation, using the optimal eigenvalue correction yields a tighter approximation to the full-matrix quantity compared to Shampoo or CASPR. It remains an open theoretical question whether a tighter Frobenius norm approximation can yield a tighter regret bound compared to Shampoo and CASPR. For example, one can obtain a tighter regret bound than Shampoo by only considering one-sided Shampoo, which is not generally a better approximation to full-matrix AdaGrad (Xie et al., 2025; An et al., 2025).

<sup>8</sup> $\mathbb{D}^d$  denotes the set of  $d \times d$  diagonal matrices.

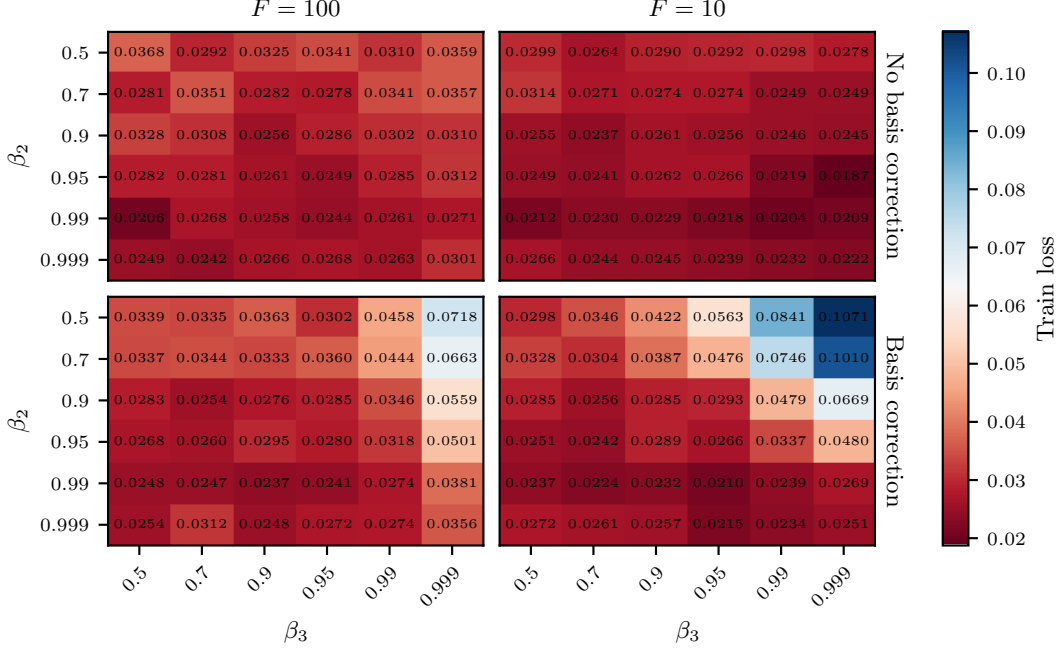


Figure 6: Decoupling the exponential moving average for the eigenbasis ( $\beta_2$ ) and eigenvalues ( $\beta_3$ ) for different eigendecomposition frequencies ( $F$ ). We can observe a remarkable invariance to the choice of  $\beta_2$  and  $\beta_3$ . Interestingly, the correction for the change of bases seems to *hurt* performance overall and especially for low  $\beta_2$ , high  $\beta_3$ , and low  $F$  values – a pattern that we might expect *without* the correction.

## D.2 Basis-aware eigenvalue correction

Despite its optimality, computing  $D^*$  for cases 2 and 3 in Proposition 3 is not feasible in practice since we would have to store and transform prior gradients from *all previous iterations* with  $Q_T$ , or have access to the full-matrix quantity  $C_T$ . For simplicity, we will focus on case 3, although the results generalize without loss of generality.<sup>9</sup> In contrast to the optimal eigenvalue correction, which uses a fixed basis matrix  $Q_T$  based on the most recent statistics  $L_T$  and  $R_T$ , SOAP uses potentially different basis matrices  $Q_t$  based on previous statistics  $L_t$  and  $R_t$  available at every step  $t = 1, \dots, T$ :

$$D^* = (1 - \beta_2) \sum_{t=1}^T \beta_2^{T-t} \text{diag}(Q_T^T g_t)^{\odot 2} \approx (1 - \beta_2) \sum_{t=1}^T \beta_2^{T-t} \text{diag}(Q_t^T g_t)^{\odot 2} =: \hat{D}_T. \quad (20)$$

Intuitively, this means that the eigenvalue correction is accumulated inconsistently *across different coordinate systems*. This can lead to a mismatch when preconditioning  $G_T$ , which is only transformed to the *current* coordinate system determined by  $Q_T$ . When the basis remains approximately constant, i.e.,  $Q_T \approx Q_t$  for all  $t$ , Equation (20) can be a tight approximation and  $D^* \approx D_T$ .

Note that the naive eigenvalue correction may be approximately correct, i.e. the basis is approximately constant, when the basis is updated infrequently, but this can be a poor approximation overall if  $Q$  does not approximate the changing eigenbasis of  $C$ , thereby increasing the approximation error. The approximation potentially becomes milder for case 3 because the terms in the sum in Equation (20) are down-weighted by  $\beta_2^{T-t}$  through the exponential moving average. Therefore, depending on  $\beta_2$ , the contribution from the eigenvalue correction statistic in previous coordinate systems might be negligible. However, this is not the case for case 2, where all terms are weighted equally.

<sup>9</sup>To address case 2, simply drop  $1 - \beta_2$  and  $\beta_2^{T-t}$ .

In order to address the theory-practice gap between the naive eigenvalue correction (used in SOAP) and the optimal correction in Frobenius norm, we first observe that

$$\begin{aligned}
D^* &= (1 - \beta_2) \sum_{t=1}^T \beta_2^{T-t} \text{diag}(\mathbf{Q}^\top \mathbf{g}_t)^{\odot 2} \\
&= (1 - \beta_2) \sum_{t=1}^T \beta_2^{T-t} \text{diag}(\mathbf{Q}_T^\top \mathbf{g}_t \mathbf{g}_t^\top \mathbf{Q}_T) \\
&= \text{diag}(\mathbf{Q}_T^\top ((1 - \beta_2) \sum_{t=1}^T \beta_2^{T-t} \mathbf{g}_t \mathbf{g}_t^\top) \mathbf{Q}_T) \\
&= \text{diag}(\mathbf{Q}_T^\top \mathbf{C}_T \mathbf{Q}_T) =: \text{diag}(\hat{\mathbf{C}}_T),
\end{aligned} \tag{21}$$

with  $\hat{\mathbf{C}}_T = \mathbf{Q}_T^\top \mathbf{C}_T \mathbf{Q}_T$ . Since  $\mathbf{Q}_T$  is orthogonal, we can recursively write

$$\begin{aligned}
D^* &= \text{diag}(\hat{\mathbf{C}}_T) = \text{diag}(\mathbf{Q}_T^\top (\beta_2 \mathbf{C}_{T-1} + (1 - \beta_2) \mathbf{g}_T \mathbf{g}_T^\top) \mathbf{Q}_T) \\
&= \text{diag}(\beta_2 \mathbf{Q}_T^\top \mathbf{C}_{T-1} \mathbf{Q}_T + (1 - \beta_2) \mathbf{Q}_T^\top \mathbf{g}_T \mathbf{g}_T^\top \mathbf{Q}_T) \\
&= \text{diag}(\beta_2 \mathbf{Q}_T^\top \mathbf{Q}_{T-1} \hat{\mathbf{C}}_{T-1} \mathbf{Q}_{T-1}^\top \mathbf{Q}_T + (1 - \beta_2) \mathbf{Q}_T^\top \mathbf{g}_T \mathbf{g}_T^\top \mathbf{Q}_T) \\
&= \beta_2 \text{diag}(\mathbf{R}_{T,T-1} \hat{\mathbf{C}}_{T-1} \mathbf{R}_{T,T-1}^\top) + (1 - \beta_2) \text{diag}(\mathbf{Q}_T^\top \mathbf{g}_T)^{\odot 2},
\end{aligned} \tag{22}$$

where  $\mathbf{R}_{T,T-1} := \mathbf{Q}_T^\top \mathbf{Q}_{T-1}$  is the transition matrix between different bases.

While this is the exact expression for our desired quantity, it requires keeping track of the full matrix  $\hat{\mathbf{C}}_{T-1}$  to compute  $\text{diag}(\mathbf{R}_{T,T-1} \hat{\mathbf{C}}_{T-1} \mathbf{R}_{T,T-1}^\top)$ , which is not tractable. Since we explicitly construct  $\mathbf{Q}_{T-1}$  to be close to the best Kronecker-factored basis for  $\mathbf{C}_{T-1}$  through the choice of the Shampoo preconditioner with  $\mathbf{L}_{T-1}$  and  $\mathbf{R}_{T-1}$ , we make the additional assumption that  $\hat{\mathbf{C}}_{T-1}$  is approximately diagonal, i.e.,  $\hat{\mathbf{C}}_{T-1} \approx \text{diag}(\hat{\mathbf{C}}_{T-1}) = \text{diag}(\mathbf{v}_{T-1}^{\text{corrected}})$ .

Substituting this back into the recursive equation above, we have that

$$\begin{aligned}
D^* &= \text{diag}(\hat{\mathbf{C}}_T) \approx \beta_2 \text{diag}(\mathbf{R}_{T,T-1} \text{diag}(\mathbf{v}_{T-1}^{\text{corrected}}) \mathbf{R}_{T,T-1}^\top) + (1 - \beta_2) \text{diag}(\mathbf{Q}_T^\top \mathbf{g}_T)^{\odot 2} \\
&= \beta_2 \text{diag}(\mathbf{R}_{T,T-1}^{\odot 2} \mathbf{v}_{T-1}^{\text{corrected}}) + (1 - \beta_2) \text{diag}(\mathbf{Q}_T^\top \mathbf{g}_T)^{\odot 2} \\
&= \text{diag}(\mathbf{v}_T^{\text{corrected}}).
\end{aligned} \tag{23}$$

This gives a recursive update rule that, in contrast to the naive solution, accounts for the changes of bases between iterations. This also recovers the exact solution when  $\mathbf{Q}_T = \mathbf{Q}_t$  for all  $t$  since  $\mathbf{R}_{t,t-1} = \mathbf{I}$ . This correction for the changing basis has a similar motivation to and resembles parts of the LDAdam algorithm (Robert et al., 2024).

We design an experiment to empirically test whether the implicit approximation in Equation (20) helps in practice, and find that interestingly, the correction appears to hurt performance in the settings where we would expect it to help, see Figure 6. A satisfying explanation of this phenomenon remains an open question.

## E Additional experimental details and results

For all experiments we used  $1 \times$  NVIDIA A100 80GB GPU per run, with the exception of the ImageNet ViT experiments, for which we used  $4 \times$  NVIDIA A100 80GB GPUs per run. All of the experiments were conducted on an internal compute cluster and we estimate that the total required compute was around 1440 GPU hours or 60 days. We ran additional exploratory experiments not reported in this paper which increases the total compute cost of the project.

### E.1 Imagewoof experimental details

We use the Imagewoof dataset.<sup>10</sup> All models are trained with cross entropy loss for 100 epochs, using a learning rate schedule consisting of a linear warmup for 353 steps followed by cosine decay. We use

<sup>10</sup>The Imagewoof dataset is available at <https://github.com/fastai/imagenette>.

a batch size of 128, randomized cropping and horizontal flips as data augmentation, and the default settings for  $\beta_1 = 0.9$  and  $\beta_2 = 0.999$ .

For the vision transformer (ViT) model, we use SimpleViT (Beyer et al., 2022) with patch size 16, 6 heads, a depth of 12 layers, an MLP dimension of 1536, dimension of 384, gradient clipping with threshold 1, and weight decay of  $10^{-4}$ . For the ConvNeXt V2 architecture (Woo et al., 2023) we use weight decay of 0.05 and drop paths with rate 0.1.

For Figure 2, we fix  $\epsilon = 10^{-10}$  and sweep the following learning rates  $\alpha$ :<sup>11</sup>

- Vision transformer
  - AdamW:  $\alpha \in \{10^{-4}, 3 \cdot 10^{-4}, 6 \cdot 10^{-4}, 10^{-3}, 3 \cdot 10^{-3}, 6 \cdot 10^{-3}, 10^{-2}\}$
  - Shampoo with grafting:  $\alpha \in \{10^{-4}, 3 \cdot 10^{-4}, 10^{-3}, 3 \cdot 10^{-3}\}$
  - Shampoo:  $\alpha \in \{3 \cdot 10^{-3}, 6 \cdot 10^{-3}, 10^{-2}, 3 \cdot 10^{-3}\}$
  - Shampoo<sup>2</sup> with trace scaling:  $\alpha \in \{10^{-4}, 3 \cdot 10^{-4}, 3 \cdot 10^{-3}\}$
  - EShampoo:  $\alpha \in \{10^{-4}, 3 \cdot 10^{-4}, 10^{-3}, 3 \cdot 10^{-3}\}$
- ConvNeXt V2
  - AdamW:  $\alpha \in \{10^{-4}, 3 \cdot 10^{-4}, 6 \cdot 10^{-4}, 10^{-3}, 3 \cdot 10^{-3}, 6 \cdot 10^{-3}, 10^{-2}\}$
  - Shampoo with grafting:  $\alpha \in \{10^{-4}, 3 \cdot 10^{-4}, 10^{-3}, 3 \cdot 10^{-3}, 10^{-2}\}$
  - Shampoo:  $\alpha \in \{10^{-4}, 3 \cdot 10^{-4}, 10^{-3}, 3 \cdot 10^{-3}\}$
  - Shampoo<sup>2</sup> with trace scaling:  $\alpha \in \{10^{-4}, 3 \cdot 10^{-4}, 10^{-3}\}$
  - EShampoo:  $\alpha \in \{10^{-4}, 3 \cdot 10^{-4}, 10^{-3}, 3 \cdot 10^{-3}, 10^{-2}\}$

For EShampoo in Figure 3, Figure 4, and Figure 5 we use the learning rate  $\alpha = 6 \cdot 10^{-4}$  and  $\epsilon = 10^{-10}$ .

## E.2 AlgoPerf workloads

We follow the standard AlgoPerf setup and consider wall-clock time to pre-specified validation metric targets. See Dahl et al. (2023) and Kasimbeg et al. (2025) for more details on the AlgoPerf benchmark.<sup>12</sup> The FastMRI dataset can be attributed to Knoll et al. (2020); Zbontar et al. (2019), the ImageNet dataset to Krizhevsky et al. (2012), and the OGBG dataset to Hu et al. (2021).

We choose this specific subset of the workloads because (1) we want to include a larger scale vision transformer (ImageNet ViT), an architecture we use in the small-scale experiments, (2) the FastMRI and OGBG workloads share the same hyperparameter settings with the Imagenet ViT workload, hence excluding them as a confounding factor, and (3) the  $\beta_2$  used for these workloads is the smallest among all hyperparameter settings of the winning Shampoo submission, resulting in the fastest moving average and thereby potentially faster changing eigenbases.

We run the winning Shampoo submission with Adam grafting,  $F = 100$ , and the best hyperparameter setting for each workload.<sup>13</sup> For EShampoo, we use the same best-performing hyperparameter setting from Shampoo but turn off learning rate grafting from Adam, and modify  $F$  and  $\tau$ .

<sup>11</sup>We fixed  $\epsilon$  based on a wide sweep over  $\alpha$  and  $\epsilon$  for AdamW. We also use this  $\epsilon$  when grafting from Adam.

<sup>12</sup>The benchmark code is available at <https://github.com/mlcommons/algorithmic-efficiency/>.

<sup>13</sup>The submission is available at [https://github.com/mlcommons/submissions\\_algorithms/tree/main/previous\\_leaderboards/algoperf\\_v05/submissions/external\\_tuning/shampoo\\_submission](https://github.com/mlcommons/submissions_algorithms/tree/main/previous_leaderboards/algoperf_v05/submissions/external_tuning/shampoo_submission).

<sup>15</sup>This wall-clock time statistic seems to be negatively impacted by either an issue with the AlgoPerf code or the hardware setup.

<sup>15</sup>Runs failed due to <https://github.com/mlcommons/algorithmic-efficiency/issues/866>.

Table 3: Results for all considered settings on a subset of the AlgoPerf workloads. We show the mean and standard error of the steps and time to the targets across the runs that actually hit the targets.

Workload	Shampoo Variant	Hits Targets	Steps	Time [min]
FastMRI	Adam grafting ( $F = 100$ )	4/5	$4301 \pm 109$	$13.96 \pm 0.44$
	$C^{\text{EShampoo}}$ ( $F = 100$ )	5/5	$2536 \pm 66$	$10.44 \pm 0.21$
	$C^{\text{EShampoo}}$ ( $F = 50$ )	5/5	$2578 \pm 86$	$10.86 \pm 0.27$
	$C^{\text{EShampoo}}$ ( $F = 10$ )	5/5	$2311 \pm 73$	$14.93 \pm 1.97$
	$C^{\text{EShampoo}}$ ( $F = 1$ )	5/5	$2101 \pm 31$	$35.34 \pm 0.70$
	$C^{\text{EShampoo}}$ ( $\tau = 0.1, F = 100$ )	5/5	$2553 \pm 154$	$16.33 \pm 2.10^{14}$
	$C^{\text{EShampoo}}$ ( $\tau = 0.1, F = 50$ )	5/5	$2468 \pm 145$	$10.81 \pm 0.72$
	$C^{\text{EShampoo}}$ ( $\tau = 0.1, F = 10$ )	5/5	$2420 \pm 92$	$10.76 \pm 0.73$
	$C^{\text{EShampoo}}$ ( $\tau = 0.1, F = 1$ )	5/5	$2367 \pm 96$	$10.93 \pm 0.42$
	$C^{\text{EShampoo}}$ ( $\tau = 0.01, F = 1$ )	5/5	$2208 \pm 41$	$27.43 \pm 0.49$
ImageNet ViT	Adam grafting ( $F = 100$ )	1/1	79907	894.27
	$C^{\text{EShampoo}}$ ( $F = 100$ )	1/1	76226	894.85
	$C^{\text{EShampoo}}$ ( $F = 10$ )	1/1	73237	1160.53
	$C^{\text{EShampoo}}$ ( $\tau = 0.1, F = 100$ )	1/1	74010	852.66
	$C^{\text{EShampoo}}$ ( $\tau = 0.1, F = 50$ )	1/1	77459	935.89
	$C^{\text{EShampoo}}$ ( $\tau = 0.01, F = 10$ )	1/1	75841	1188.76
OGBG	Adam grafting ( $F = 100$ )	2/5	$12574 \pm 708$	$39.20 \pm 1.88$
	$C^{\text{EShampoo}}$ ( $F = 100$ )	3/5	$8320 \pm 1203$	$33.02 \pm 4.05$
	$C^{\text{EShampoo}}$ ( $F = 50$ )	5/5	$7173 \pm 443$	$26.17 \pm 1.31$
	$C^{\text{EShampoo}}$ ( $F = 10$ )	3/5	$6645 \pm 357$	$37.55 \pm 1.74$
	$C^{\text{EShampoo}}$ ( $F = 1$ ) <sup>15</sup>	–	–	–
	$C^{\text{EShampoo}}$ ( $\tau = 0.1, F = 100$ )	4/5	$8047 \pm 369$	$27.60 \pm 1.15$
	$C^{\text{EShampoo}}$ ( $\tau = 0.1, F = 50$ )	5/5	$7117 \pm 328$	$27.55 \pm 3.49$
	$C^{\text{EShampoo}}$ ( $\tau = 0.1, F = 10$ )	5/5	$7151 \pm 416$	$29.11 \pm 1.98$
	$C^{\text{EShampoo}}$ ( $\tau = 0.1, F = 1$ )	5/5	$6758 \pm 273$	$34.16 \pm 1.65$
	$C^{\text{EShampoo}}$ ( $\tau = 0.01, F = 10$ )	2/5	$7234 \pm 361$	$39.15 \pm 2.01$

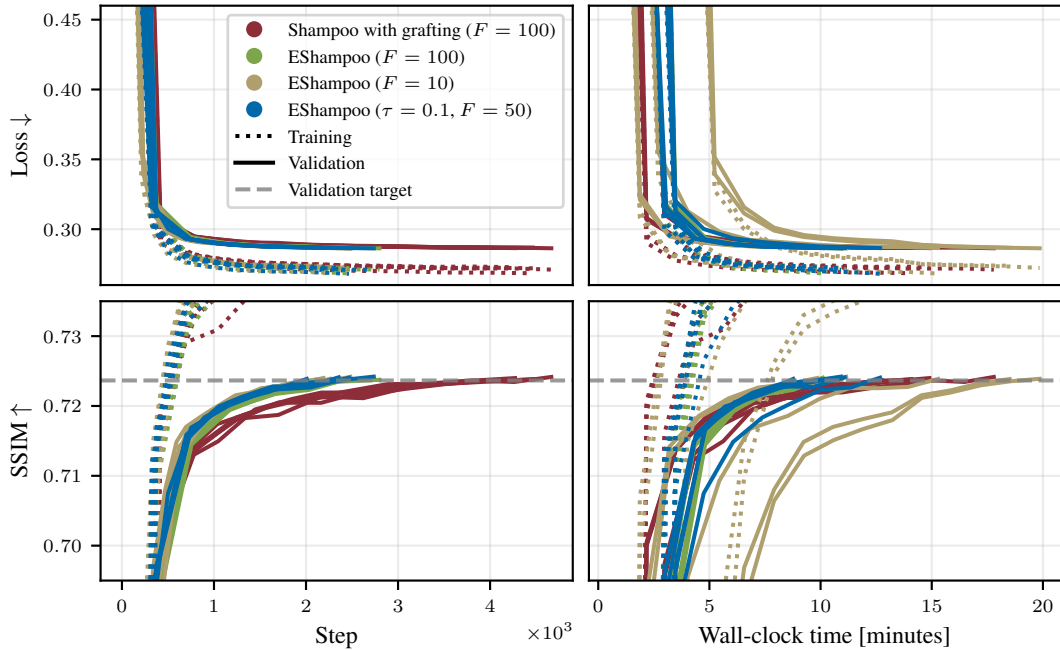


Figure 7: FastMRI AlgoPerf workload.

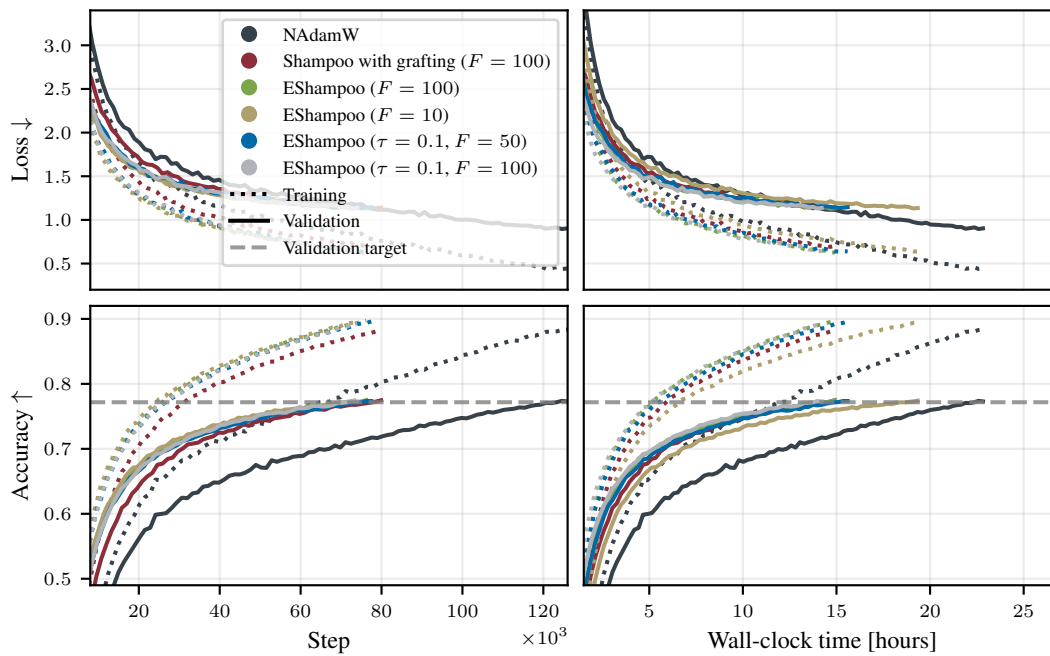


Figure 8: ImageNet ViT AlgoPerf workload.

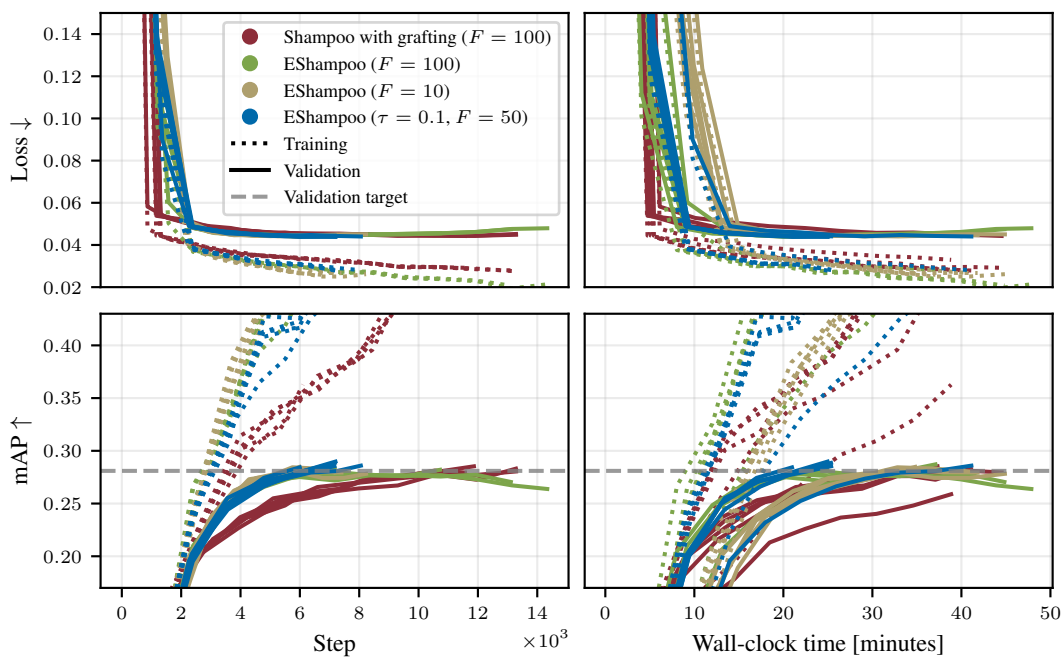


Figure 9: OGBG AlgoPerf workload.